AD-A079 905 AIR FORCE INST OF TECH WRIGHT-PATTERSON AFB OH SCHOO--ETC F/G 11/4
EFFECT OF IMPERFECTIONS ON THE COLLAPSE OF RECTANGULAR PLATES U--ETC(U)
DEC 79 L G PECK
UNCLASSIFIED AFIT/GAE/AA/79D-14 NL

END
DATE FILMED
2 -80
DDC

AFIT/GAE/AA/79D-14

EFFECT OF IMPERFECTIONS ON THE COLLAPSE OF RECTANGULAR PLATES USING VARIATIONAL CALCULUS

THESIS

AFIT/GAE/AA/79D-14 LYLE G. PECK
CAPT USAF

AFIT/GAE/AA/79D-14

Effect of Imperfections on the Collapse of Rectangular Plates Using Variational Calculus

THESIS

Presented to the Faculty of the School of Engineering
of the Air Force Institute of Technology
Air University
in Partial Fulfillment of the
Requirement for the Degree of
Master of Science

by

Lyle G. Peck, B.S., M.S.
Captain USAF
Graduate Aeronautical Engineering

December 1979

Preface

Classical plate analysis generally assumes initially perfect plates when considering collapse due to inplane stresses. This report incorporates the assumption of initial imperfections in geometry in an analytical investigation of collapse involving elastic, elastic-plastic and orthotropic plates.

I wish to express my sincere appreciation to Dr. Anthony Palazotto for his valuable instruction, encouragement and timely advice. I particularly want to thank my wife and family for their patience and understanding during my preoccupation with this thesis.

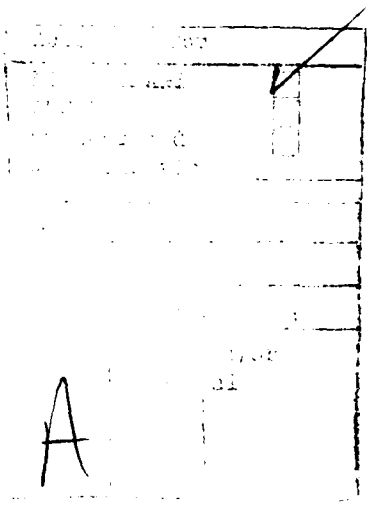

Contents

List of Figures

List of Tables

Symbols

a	half dimension in the x-direction, in.
a_{ij}	coefficients in incremental algebraic equations
b	half dimension in the y-direction, in.
C_{ij}	coefficients of material constitutive equations
D_{ij}	bending stiffnesses for orthotropic material
E	Young's Modulus, lb/in^2
E_o	Remberg-Osgood material constant
E_1	Young's Modulus in longitudinal direction, lb/in^2
E_2	Young's Modulus in transverse direction, lb/in^2
E_{ij}	Green's Strain Tensor
$\dot{E}_{ij}$	incremental strain tensor
G	plastic hardening function
G_{12}	orthotropic shear modulus, lb/in^2
I^o	functional for rate problem
J_2	second invariant of the stress deviator tensor
k	Ramberg-Osgood material constant
m	number of half-sine waves in x-direction
n	number of half-sine waves in y-direction
t	thickness of plate, in.
$u, v, w,$	displacements in the x, y, z direction, in.
$u_x, u_y, u_z,$	displacements in the x, y, z direction, in.
u^o, v^o, w^o	initial displacements in the x, y, z direction, in.
$\dot{u}, \dot{v}, \dot{w}$	incremental displacements in the x, y, z direction, in.
x, y, z	load axes of plate
$1, 2, 3$	major orthotropic material axes
$\alpha_1, \alpha_2, \alpha_3,$	parameters of stress due to moment

$\dot{\alpha}_1, \dot{\alpha}_2, \dot{\alpha}_3$	incremental parameters
β^*	measure of in plane displacement, in.
$\dot{\beta}^*$	measure of incremental displacement, in.
δ^o	measure of imperfection size, in.
$\dot{\delta}$	incremental displacement parameter, in.
ε	strain
σ	stress, stress parameter
$\dot{\sigma}$	incremental stress parameter
τ_{ij}	stress, lb/in^2
τ^o_{ij}	initial stress, lb/in^2
$\dot{\tau}$	incremental stress, lb/in^2
ν	Poisson's ratio
ν_{12}	Poisson's ratio for transverse strain in the 2-direction when stress is the 1-direction

Abstract

An analysis is made of the effect of initial imperfections in geometry on the collapse of simply-supported rectangular plates. A Reissner-type variational principle is employed to evaluate the load versus lateral displacement of elastic, elastic-plastic and orthotropic plates subject to compressive loading along two edges. Imperfection size and shape, plate thickness and aspect ratio, and for orthotropic material, the ply orientation is examined. The results indicate that the load-displacement curve is sensitive to the initial imperfection, particularly for elastic-plastic materials. The effect of plate size and aspect ratio are similar for all the plates considered with the collapse stresses higher for elastic plates than for elastic-plastic plates. The effect of plasticity becomes insignificant for thin plates when compared with plates with elastic properties. In general, it can be stated that the imperfection function determines the plate's collapse load. For orthotropic plates the effect of ply orientation is significant at aspect ratios less than 1 but relatively insignificant at higher values when comparing the minimum collapse stresses. The difference is dependent upon the magnitude of the ratio of Young's moduli in the major material axes.

EFFECT OF IMPERFECTIONS ON THE COLLAPSE OF RECTANGULAR PLATES USING VARIATIONAL CALCULUS

I. Introduction

Background

The first problems in elastic instabi ty were solved over 200 years ago by Euler (1) working with the lateral buckling of compressed members. Since that time the science of structural stability has received attention by numerous individuals. Because of its application as a structural member in modern structures, the rectangular plate is of particular interest in this thesis.

In the late 1800's Bryan (2) studied plates, applying the theory to the buckling of the sides of ships. In the early 1800's Timoshenko (3) treated numerous types of loading and boundary conditions utilizing both the energy approach and the solution of the differential equations. In his 1940 work, Hill (4) constructed charts describing the critical compressive stresses for flat rectangular elastic plates. The results of the above cited work compare favorably with experimentation.

In 1942 Lundquist and Stowell (5) presented the first unified treatment of the elastic-plastic compressive buckling problem, using both the differential equations and energy methods. However, much of the classical work with elastic-

plastic plates resulted in critical compressive stresses which were significantly higher than experimental results. It was shown by Onat and Drucker (6 7) for the axially compressed cruciform column and by Neale (8) for the cylindrical shell under torsion that these theoretical stresses could be brought much closer to experimental results by including in the analysis initial geometric imperfections. Consequently, the idealization of a geometrically perfect system adopted in the classical approach no longer remains acceptable. In his work presented in 1974, Neale (9) employed the variational principle and a Ritz method incorporating imperfections into the analysis of the plastic buckling of rectangular plates. His results show much closer agreement to experimental data.

The 1960's and 1970's have seen the increasing use of composite material particularly in structures requiring high strength-to-weight ratios. These composite materials often possess orthotropic properties, and consequently modified theories for the solution of problems where composite materials are used, are required. Ashton and Whitney (10) present the theoretical development and solutions for plates fabricated of thin layers of anisotropic material. Jones (11) and Chamis (12) present the major aspects of the science and technology of composite materials that are the basics of todays technology.

These three types of material, elastic, elastic-plastic

and orthotropic, form the basis of the spectrum of material properties. With the exception of Neale's work with elastic-plastic plates, little has been published that illustrates the effect of initial geometric imperfections on the collapse of rectangular plates. Consequently, it is this subject to which this thesis is devoted.

Purpose

The purpose of this thesis is to examine analytically, the effect of small and consequently unavoidable imperfections in geometry on the collapse of simply supported rectangular plates subject to in-plane compression along two edges. Three different types of material, elastic, elastic-plastic, and orthotropic, will be compared and the effect of aspect ratio (i.e. length/width), length/thickness, shape of initial imperfections, size of imperfection and for the orthotropic case, ply orientation, will be examined.

The analytical technique that will be used consists of the formulation of a "rate" or incremental boundary-value problem, which can be solved in an approximate manner using a variational principle (13) in conjunction with the method of Ritz. A stepwise solution of this rate problem furnishes the pertinent load-deformation behavior (9). Using this formulation the problem reduces to a set of five algebraic equations which can be solved incrementally using a minimum of computer time or possibly an advanced hand calculator or desk computer.

Scope

All the plates examined are 0.1 inches thick. Length-to-thickness ratios vary from 10 to 400 and aspect ratios vary from 0.5 to 4.0. For each case an initial imperfection of 10^{-6}, 10^{-4}, 10^{-2} inches is evaluated. The effect of the shape of the imperfection is evaluated using m and n of 1, 3, 5, where m is the number of half sine waves in the x-direction and n is the number of half sine waves in the y-direction. For further explanation see results and discussion. For the orthotropic case, a single ply with fiber orientation at 0^{o} and 90^{o} with respect to the applied load is evaluated.

Computer values of critical load are compared with Timoshenko (3) for the elastic case, Neale (9) for the elastic-plastic case and Chamis (14), and Mandell (15) for the orthotropic case.

II. Theory

Since the case of elastic-plastic material is the most general of the three materials, the theoretical analysis will center on plasticity with appropriate modification made for the elastic and orthotropic cases.

Reissner (16 - 19) provided the starting point for the derivation with his general variational theorem for stresses and displacements. Reissner's theorem presents the equilibrium equations and stress-strain relations as Euler Equations of the variational problem. Boundary conditions for stresses and displacements are the natural boundary conditions. The method permits independent selection of both the stress distributions and displacement quantities in the approximate solution to the boundary-value problem.

Since the undeformed configuration of the material is often used as the reference frame, the Lagrangian form of the equations is more appropriate than the Eulerian form, which refers to the deformed configuration. In conjunction with this, suitable definitions of stress and strain are the Kirchhoff's stress tensor and Green's strain tensor (20).

General expressions for the Euler Equations of the variational principal and natural boundary conditions can be developed using the aforementioned relations. A complete derivation can be found in reference (13). These relations are subsequently applied to rectangular plates. In accord-

ance with Neale's work (9), rectangular cartesian coordinates x, y describe the location of points on the midplane of the plate and z describes the distance from the midplane, as shown in figure 1. By assuming normal plane surfaces remain plane, the displacement components are specified as follows:

$$u_x = u - z\frac{\partial w}{\partial x}$$

$$u_y = v - z\frac{\partial w}{\partial y} \qquad (1)$$

$$u_z = w$$

where u, v, w are the displacement components in the x, y, z directions respectively. The Green strains associated with these displacements are (20):

$$E_{xx} = \frac{\partial u}{\partial x} - z\frac{\partial^2 w}{\partial x^2} + \tfrac{1}{2}\left(\frac{\partial w}{\partial x}\right)^2$$

$$E_{yy} = \frac{\partial v}{\partial y} - z\frac{\partial^2 w}{\partial y^2} + \tfrac{1}{2}\left(\frac{\partial w}{\partial y}\right)^2$$

$$E_{xy} = \tfrac{1}{2}\left[\frac{\partial u}{\partial y} + \frac{\partial v}{\partial x} - 2z\frac{\partial^2 w}{\partial x \partial y} + \frac{\partial w}{\partial x}\frac{\partial w}{\partial y}\right] \qquad (2)$$

The products and squares of the derivatives incorporating the transverse displacement w, are the only nonlinear terms retained. The strain rates can be determined from equation (2) yielding results which assume homogeneity in time.

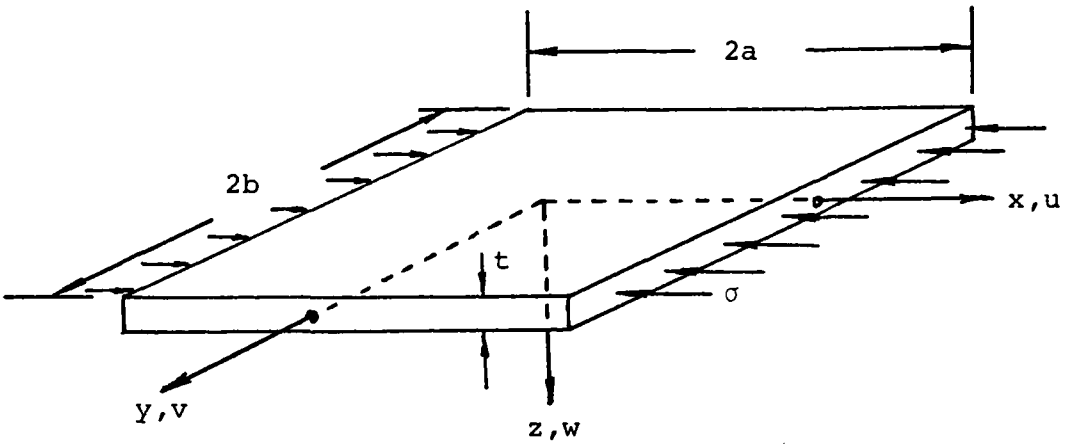

Figure 1. Plate Loading and Geometry

$$\dot{E}_{xx} = \frac{\partial \dot{u}}{\partial x} - z\frac{\partial^2 \dot{w}}{\partial x^2} + \frac{\partial w}{\partial x}\frac{\partial \dot{w}}{\partial x}$$

$$\dot{E}_{yy} = \frac{\partial \dot{v}}{\partial y} - z\frac{\partial^2 \dot{w}}{\partial y^2} + \frac{\partial w}{\partial y}\frac{\partial \dot{w}}{\partial y}$$

$$\dot{E}_{xy} = \tfrac{1}{2}\left[\frac{\partial \dot{u}}{\partial y} + \frac{\partial \dot{v}}{\partial x} - 2z\,\frac{\partial^2 \dot{w}}{\partial x \partial y} + \frac{\partial w}{\partial x}\frac{\partial \dot{w}}{\partial y} + \frac{\partial \dot{w}}{\partial x}\frac{\partial w}{\partial y}\right] \tag{3}$$

where the dot above the term, $(\dot{})$, denotes an incremental function. The incremental stress and strain constitutive equations may be stated by the following matrix expressions:

$$\begin{Bmatrix} \dot{E}_{xx} \\ \dot{E}_{yy} \\ \dot{E}_{xy} \end{Bmatrix} = \begin{bmatrix} C_{11} & C_{12} & C_{13} \\ C_{12} & C_{22} & C_{23} \\ \frac{C_{13}}{2} & \frac{C_{23}}{2} & C_{33} \end{bmatrix} \begin{Bmatrix} \dot{\tau}_{xx} \\ \dot{\tau}_{yy} \\ \dot{\tau}_{xy} \end{Bmatrix} \tag{4}$$

in which the quantities τ_{xz}, τ_{yz}, τ_{zz} are considered negligible by the assumption of plane stress.

For an isotropic solid characterized by elastic-plastic response incorporating the Von Mises incremental theory, one may obtain the C_{ij} coefficients in Eq. (4) (21):

$$C_{11} = \frac{1}{E} + \frac{G}{9}\left(2\tau_{xx} - \tau_{yy}\right)^2$$

$$C_{12} = \frac{-\nu}{E} + \frac{G}{9}\left(2\tau_{xx} - \tau_{yy}\right)\left(2\tau_{yy} - \tau_{xx}\right)$$

$$C_{13} = \frac{2G}{3}\,\tau_{xy}\left(2\tau_{xx} - \tau_{yy}\right)$$

$$C_{22} = \frac{1}{E} + \frac{G}{9}\left(2\tau_{yy} - \tau_{xx}\right)^2$$

$$C_{23} = \frac{2G}{3}\,\tau_{xy}\left(2\tau_{yy} - \tau_{xx}\right)$$

$$C_{33} = \frac{1+\nu}{E} + 2G\tau_{xy}^2 \tag{5}$$

where E is Young's modulus and ν is Poisson's ratio. If it is assumed that the uniaxial stress-strain can be described by a Ramberg-Osgood relation of the form

$$E_{xx} = \frac{\tau_{xx}}{E} + \left(\frac{\tau_{xx}}{E_0}\right)^k \tag{6}$$

where E_0 and k are material constants, then for plastic loading, the hardening function G can be written as

$$G = \frac{3k\left(\sqrt{3J_2}\right)^{k-1}}{4J_2 E_0^{\,k}} \tag{7}$$

The quantity J_2 is stated as (21),

$$J_2 = 1/3(\tau_{xx}^2 - \tau_{xx}\,\tau_{yy} + \tau_{yy}^2) + \tau_{xy}^2 \tag{8}$$

To simplify the analysis, k is taken to be 3 so that the hardening function becomes

$$G = 27/4E_0^{\,3} \tag{9}$$

which remains constant throughout the load application. It may be observed that the strain increments in Eq(4) are functions of the known stress components and a set of new incremental stresses. This set of constitutive relationships is known as the Prandtl-Reuss flow law of plasticity.

Likewise when evaluating an isotropic, elastic material under plane stress, matrix C_{ij} becomes (22):

$$C_{11} = \frac{1}{E}, \quad C_{12} = \frac{-\nu}{E}, \quad C_{13} = 0$$

$$C_{21} = \frac{-\nu}{E}, \quad C_{22} = \frac{1}{E}, \quad C_{23} = 0$$

$$C_{33} = \frac{1+\nu}{E} \tag{10}$$

As an added feature to the use of Eq(4), one may modify the expressions in order to account for orthotropic material properties associated with composites. Using θ as the angle between the major material axis and the x-axis, the coefficients may be stated as (11):

$$C_{11} = S_{11} \cos^4\theta + (2S_{12} + S_{66}) \sin^2\theta \cos^2\theta + S_{22} \sin^4\theta$$

$$C_{12} = S_{12}(\sin^4\theta + \cos^4\theta) + (S_{11} + S_{22} - S_{66}) \sin^2\theta \cos^2\theta$$

$$C_{13} = (2S_{11} - 2S_{12} - S_{66}) \sin\theta \cos^3\theta - (2S_{22} - 2S_{12} - S_{66}) (\sin^3\theta \cos\theta)$$

$$C_{22} = S_{11} \sin^4\theta + (2S_{12} + S_{66}) \sin^2\theta \cos^2\theta + S_{22} \cos^4\theta$$

$$C_{23} = (2S_{11} - 2S_{12} - S_{66}) \sin^3\theta \cos\theta - (2S_{22} - 2S_{12} - S_{66}) (\sin\theta \cos^3\theta)$$

$$C_{33} = (2S_{11} + 2S_{22} - 4S_{12} - S_{66}) \sin^2\theta \cos^2\theta + \tfrac{1}{2} S_{66} (\sin^4\theta + \cos^4\theta) \tag{11}$$

where

$$S_{11} = \frac{1}{E_1}$$

$$S_{12} = \frac{-\nu_{12}}{E_1} = \frac{-\nu_{21}}{E_2}$$

$$S_{22} = \frac{1}{E_2}$$

$$S_{66} = \frac{1}{G_{12}} \tag{12}$$

The quantities E_1 and E_2 are the Young's moduli in the longitudinal and transverse material directions. The term ν_{ij} is Poisson's ratio for transverse strain in the j-direction when stressed in the i-direction. G_{12} is the shear modulus in the 1-2 plane.

Thus, Eq. (4) is useful for any general material as long as some constitutive relationship can be found.

Formulation of Rate Boundary-Value Problem for Plates

Applying the general solution of the rate boundary-value problem, the functional I^o can be stated for a simply supported rectangular plate as (9)

$$I^o = \int_{-t/2}^{t/2} \int_{-b}^{b} \int_{-a}^{a} \dot{\tau}_{ij} \dot{E}_{ij} + \tfrac{1}{2} \tau_{ij} v_{k,i} v_{k,j} - W(\dot{\tau}) \, dxdydz \tag{13}$$

where $\dot{\tau}_{ij} \dot{E}_{ij} = \dot{\tau}_{xx} \dot{E}_{xx} + 2\dot{\tau}_{xy} \dot{E}_{xy} + \dot{\tau}_{yy} \dot{E}_{yy}$

$$\tau_{ij} v_{k,i} v_{k,j} = \tau_{xx} \left(\frac{\partial \dot{w}}{\partial x}\right)^2 + 2\tau_{xy} \frac{\partial \dot{w}}{\partial x} \frac{\partial \dot{w}}{\partial y} + \tau_{yy} \left(\frac{\partial \dot{w}}{\partial y}\right)^2$$

$$2 W(\dot{\tau}) = C_{11} \dot{\tau}_{xx}^2 + 2C_{12} \dot{\tau}_{xx} \dot{\tau}_{yy} + C_{22} \dot{\tau}_{yy}^2 + 2C_{13} \dot{\tau}_{xx} \dot{\tau}_{xy} + 2 C_{23} \dot{\tau}_{xy} \dot{\tau}_{yy} + 2 C_{33} \dot{\tau}_{xy}^2 \tag{14}$$

with C_{ij} specified in equations (5), (6), (11) for elastic-plastic, elastic and orthotropic materials respectively.

The general variational principal states the functional I^o is stationary in the vicinity of the solution. The boundary value problem consists of determining the incremental stress

and displacement functions, $\dot{\tau}_{xx}$, $\dot{\tau}_{yy}$, $\dot{\tau}_{xy}$, $\dot{u}$, $\dot{v}$, $\dot{w}$, which satisfy the boundary conditions corresponding to the specified edge displacements. Using the method of Ritz, an approximate solution for these incremental quantities can be obtained.

The problem considered is one in which a u displacement is initiated in a plate characterized by a geometric imperfection of the form

$$w^o = \delta^o \, t \cos \frac{m\pi x}{2a} \cos \frac{n\pi y}{2b} \tag{15}$$

where δ^o is a measure of the size of the imperfection and t is the plate thickness. All other initial stresses and displacements are zero.

$$\tau^o_{xx} = \tau^o_{yy} = \tau^o_{xy} = u^o = v^o = 0 \tag{16}$$

The approximate form of the stresses are taken to be

$$\begin{aligned}
\dot{\tau}_{xx} &= -\dot{\sigma} + \dot{\alpha}_1 \frac{z}{t} \cos \frac{m\pi x}{2a} \cos \frac{n\pi y}{2b} \\
\dot{\tau}_{yy} &= \dot{\alpha}_2 \frac{z}{t} \cos \frac{m\pi x}{2a} \cos \frac{n\pi y}{2b} \\
\dot{\tau}_{xy} &= \dot{\alpha}_3 \frac{z}{t} \sin \frac{m\pi x}{2a} \sin \frac{n\pi y}{2b}
\end{aligned} \tag{17}$$

The incremental edge displacements can be specified as

$$\begin{aligned}
\dot{u} &= -\dot{\beta}^* x \\
\dot{v} &= 0 \\
\dot{w} &= \dot{\delta} t \cos \frac{m\pi x}{2a} \cos \frac{n\pi y}{2b}
\end{aligned} \tag{18}$$

with $\dot{\beta}^*$ being a measure of the size of the edge displacement. The observer may notice that under the above conditions, the plate is allowed to move in such a way that midplane stresses are zero in shear and the y-direction. This can only occur if the boundary conditions along y = ± b are held by a very flexible support. *In order to create* $\dot{v} = 0$ displacement, an external source is necessary to relieve any restraining τ_{yy} and τ_{xy} midplane stresses. With this artificial boundary, it is possible to totally isolate the plate's imperfections and remove post buckling stresses resulting from restrained boundaries.

The variational principal

$$\delta I^o = 0$$

yields for this problem

$$\frac{\partial I^o}{\partial \dot{\delta}} = \frac{\partial I^o}{\partial \dot{\sigma}} = \frac{\partial I^o}{\partial \dot{\alpha}_1} = \frac{\partial I^o}{\partial \dot{\alpha}_2} = \frac{\partial I^c}{\partial \dot{\alpha}_3} = 0 \qquad (20)$$

which is a system of differential equations in the unknown incremental parameters $\dot{\delta}$, $\dot{\sigma}$, $\dot{\alpha}_1$, $\dot{\alpha}_2$, $\dot{\alpha}_3$.

The stress and displacement distribution can be determined by adding the incremental quantities to the previous conditions,

$$u = \beta^* x$$

$$v = 0$$

$$w = \delta t \cos \frac{m\pi x}{2a} \cos \frac{n\pi y}{2b}$$

$$\tau_{xx} = -\sigma + \alpha_1 \frac{z}{t} \cos \frac{m\pi x}{2a} \cos \frac{n\pi y}{2b}$$

$$\tau_{yy} = \alpha_2 \frac{z}{t} \cos \frac{m\pi x}{2a} \cos \frac{n\pi y}{2b}$$

$$\tau_{xy} = \alpha_3 \frac{z}{t} \sin \frac{m\pi x}{2a} \sin \frac{n\pi y}{2b} \qquad (21)$$

Consequently, the stress and displacement at any instant of time can be determined by the interative solution of a set of five algebraic equations in $\dot{\delta}$, $\dot{\sigma}$, $\dot{\alpha}_1$, $\dot{\alpha}_2$, $\dot{\alpha}_3$. Therefore, the problem may be represented in matrix format as

$$\left[a_{ij} \quad (\delta, \sigma, \alpha_1, \alpha_2, \alpha_3) \right] \begin{bmatrix} \dot{\delta} \\ \dot{\sigma} \\ \dot{\alpha}_1 \\ \dot{\alpha}_2 \\ \dot{\alpha}_3 \end{bmatrix} = \left[b_i \right] \qquad (22)$$

with the initial conditions being

$$\delta = \delta^o$$

$$\sigma^o = \alpha_1^o = \alpha_2^o = \alpha_3^o = 0$$

Determination of a_{ij} Matrix

In order to obtain the a_{ij} coefficients, Eq's (3, 17, 18) are substituted into Eq. (14) with the required partial derivatives of Eq. (18). To obtain the C_{ij}'s, Eq's (10) or (11) are substituted into Eq. (14). Equation (14) can be developed for the elastic-plastic case by substituting Eq. (21) into Eq. (5) and then the results into Eq. (14). The resulting

expression is then introduced into Eq. (13) which produces a desired form of the functional I^{o}. It is convenient to take the variation of the function with respect to the parameters $\dot{\delta}$, $\dot{\sigma}$, $\dot{\alpha}_1$, $\dot{\alpha}_2$, $\dot{\alpha}_3$ prior to the required integrations, as several terms become zero in the derivative. Switching the order of variation and integration is possible since the integration is independent of the variables of the variation. Subsequent integration yields the desired a_{ij} coefficients.

$$\begin{aligned}
\frac{\partial I^{o}}{\partial \dot{\delta}} &= a_{11}\dot{\delta} + a_{12}\dot{\sigma} + a_{13}\dot{\alpha}_1 + a_{14}\dot{\alpha}_2 + a_{15}\dot{\alpha}_3 \\
\frac{\partial I^{o}}{\partial \dot{\sigma}} &= a_{21}\dot{\delta} + a_{22}\dot{\sigma} + a_{23}\dot{\alpha}_1 + a_{24}\dot{\alpha}_2 + a_{25}\dot{\alpha}_3 \\
\frac{\partial I^{o}}{\partial \dot{\alpha}_1} &= a_{31}\dot{\delta} + a_{32}\dot{\sigma} + a_{33}\dot{\alpha}_1 + a_{34}\dot{\alpha}_2 + a_{35}\dot{\alpha}_3 \\
\frac{\partial I^{o}}{\partial \dot{\alpha}_2} &= a_{41}\dot{\delta} + a_{42}\dot{\sigma} + a_{43}\dot{\alpha}_1 + a_{44}\dot{\alpha}_2 + a_{45}\dot{\alpha}_3 \\
\frac{\partial I^{o}}{\partial \dot{\alpha}_3} &= a_{51}\dot{\delta} + a_{52}\dot{\sigma} + a_{53}\dot{\alpha}_1 + a_{54}\dot{\alpha}_2 + a_{55}\dot{\alpha}_3
\end{aligned} \tag{23}$$

A detailed derivation and listing of the a_{ij} matrix for elastic-plastic, elastic and orthotropic materials is included in Appendix B.

At this point the problem is reduced to an iterative solution of the system of algebraic equations defined by Eq. (22). For this thesis the solution to the matrix expression uses the Fortran IV linear equation solver LEQT1F from the IMSL library. The solution of the set of linear equation, $\dot{\delta}$, $\dot{\sigma}$, $\dot{\alpha}_1$, $\dot{\alpha}_2$, $\dot{\alpha}_3$, is added to the previous values, δ, σ, α_1, α_2, α_3 and substituted in the a_{ij}

equations, resulting in new values for a_{ij} which are subsequently used in the next iteration. This procedure is continued until the load-deformation curve is determined. The number of iterations is dependent upon the size of β^*.

A significant advantage of this procedure is that the expressions for stress and displacement allow analytic integration of I^o which eliminates the necessity for performing expensive numerical integration at each step and permits the possibility of adapting the analysis to relatively simple computational devices, i.e. advanced hand calculators or desk computers.

III. Results and Discussion

This section contains a summary of results found from the different applications of this study. A computer program was created which utilized the analytical technique presented in Section II to calculate the load versus displacement data for the various plate configurations of interest.

Verification of Computer Program

Since the work by Neale on elastic-plastic plates (9) uses the same analytical technique as this thesis, his results are used as a comparison, to verify that the developed computer program produces reliable values.

Sample runs were made with square plates incorporating $2a/t$ ratios of 20, 30 and 40. The results are compiled in Table I, comparing the critical compressive loads. The critical compressive load is taken to be the point at which further increase in edge displacement results in a decrease in the compressive load, σ. It is apparent that the program produces results very favorable with those of Neale. In fact, all the solutions are equal to or lower than the published results. As is expected with a Ritz approximation, the solution approaches convergence from above and consequently the results that are lower than Neale's are assumed to be slightly closer to exact values, due to the convergence technique.

Of significant interest in the study was the solution convergence criteria. To arrive at a solution,

Table I

Comparison of Critical Compressive Loads

	2a/t					
	20		30		40	
δ^0	Neale	Thesis	Neale	Thesis	Neale	Thesis
10^{-2}	.286	.285	.211	.211	.168	.168
10^{-4}	.383	.381	.281	.280	.222	.221
10^{-6}	.448	.444	.327	.327	.257	.256

a particular increment size, β^*, was chosen and the program carried out the iterations until the stress of the ith iteration was less than the stress of the i-1 iteration. This point was taken as the relative critical stress. The step size was reduced by one-half and a new relative critical stress was found. The process continued until the jth relative critical stress fell within 1% of the j-1 relative critical stress. This point is called the critical compressive stress for the plate (see Figure 2). The choice of β^* is of course important, in that by choosing a β^* too large one obtains a curve diverging from the correct solution. On the other hand, selecting β^* too small required many more iterations than necessary to reach convergence. Since one advantage of this technique is the simplicity of the numerical iteration process, the requirement for more iterations than are needed, presents a drawback to adapting the procedure to less expensive computing devices.

Figure 3 illustrates a typical load versus displacement curve for an elastic-plastic plate with a = 1.0, b = 1.0, t = .1, E = 30 x 10^6, ν = .3 and Ramberg-Osgood material constants, from Equation (6), of E/E_0 = 300 and k = 3. The non-dimensional load σ/E_0 is plotted against the displacement of the center of the plate in the z-direction. Curves are shown for initial imperfections of 1 half-sine wave in the x and y direction, (i.e., m, n = 1), of magnitude $\delta^0 = 10^{-2}$, 10^{-4} and 10^{-6} inches.

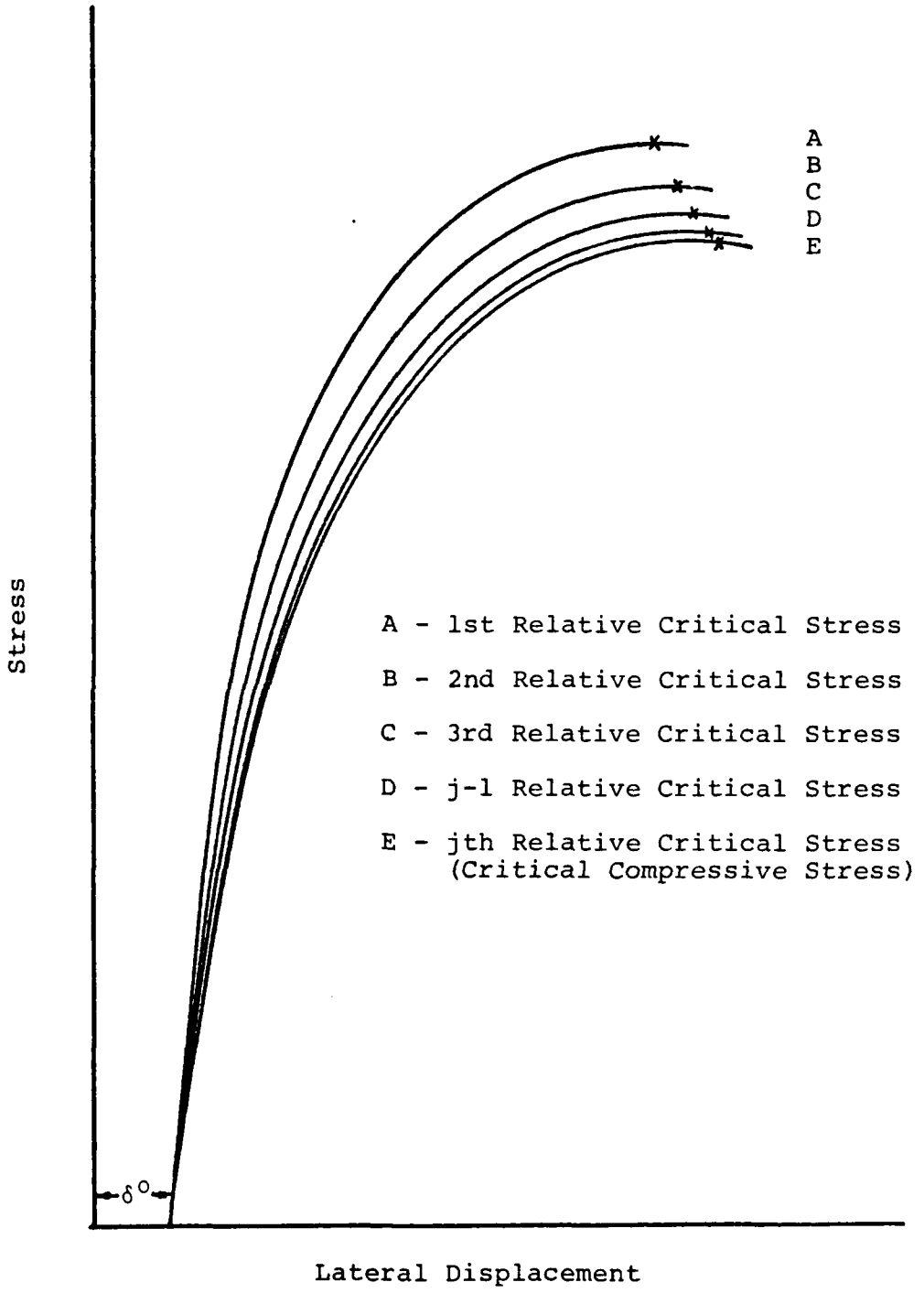

Fig. 2. Convergence to Critical Stress through Repeated Iteration

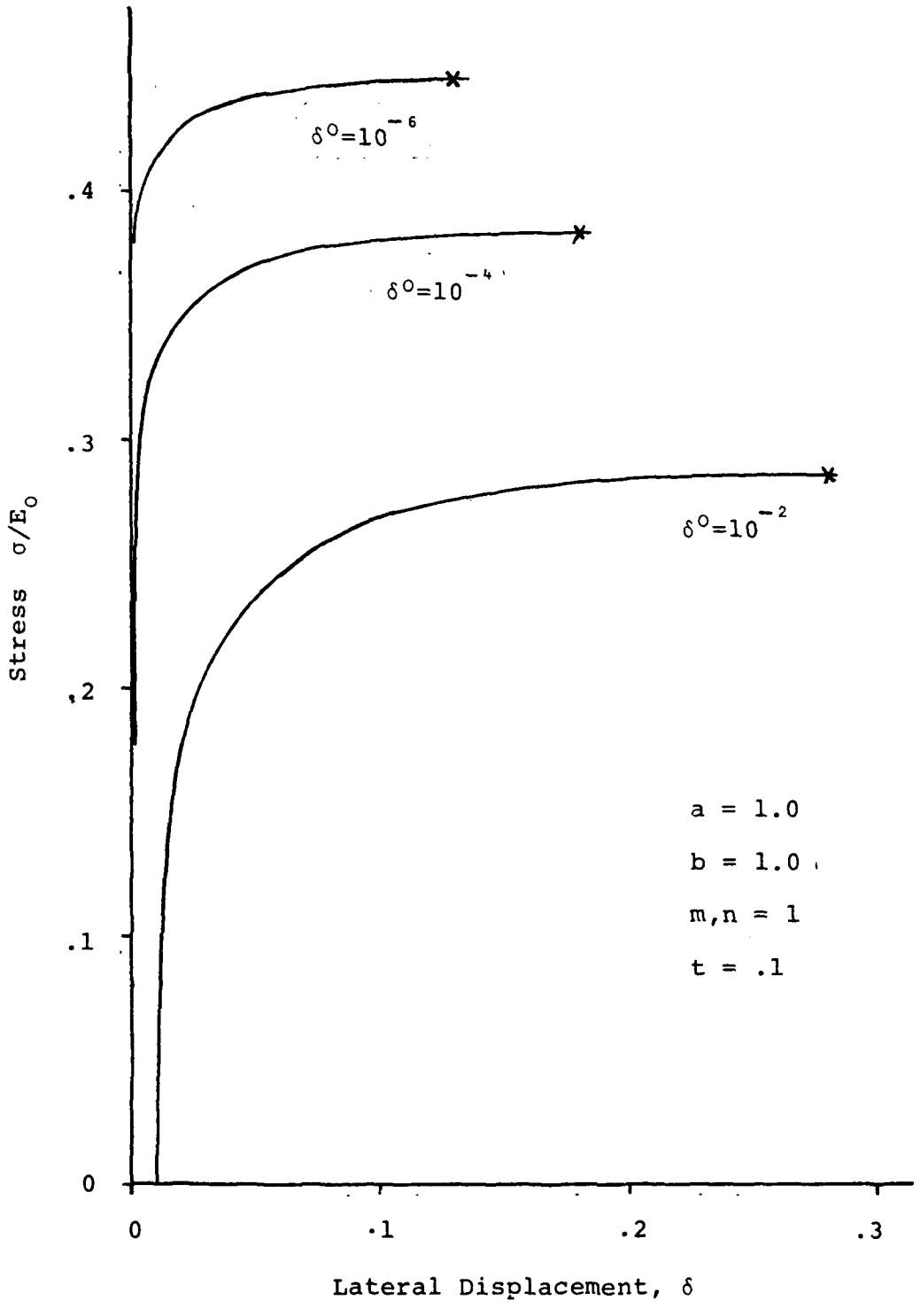

Fig. 3. Stress vs. Displacement for Typical Elastic-Plastic Material

With the above results indicating close comparison with published data, the effect of varying the parameters was evaluated.

Elastic-Plastic Materials

Load versus displacement curves were obtained for plates with 2a/t ratios of 10, 20, 40, 100, 200, 400. The shape of the individual curves are consistent with those shown in Figure 3. Increasing initial imperfection size coincides with smaller critical stress and larger displacement at collapse. Since the shape of the curves do not vary greatly from those shown, individual plots are not shown for each case. If the a and b dimensions of the plate are increased, keeping a/b equal to 1, the stress required to reach the critical stress declines rapidly for 2a/t less than 100. The rate of decrease slows and approaches zero as 2a/t becomes large, (see Figure 4). If the shape of the imperfection is changed by increasing the number of half-sine waves, the critical stress is increased significantly. For all plate sizes, a/b = 1, the minimum critical stress is found at m, n = 1. Further discussion of the effects of m and n is found later in the text.

If the ratio of length to width, a/b, is varied, a significant difference in critical stress is found depending on whether the length is held constant, (2a = constant), and the width varied, or if the width is held constant, (2b = constant). These effects are shown in Figure 5 with the

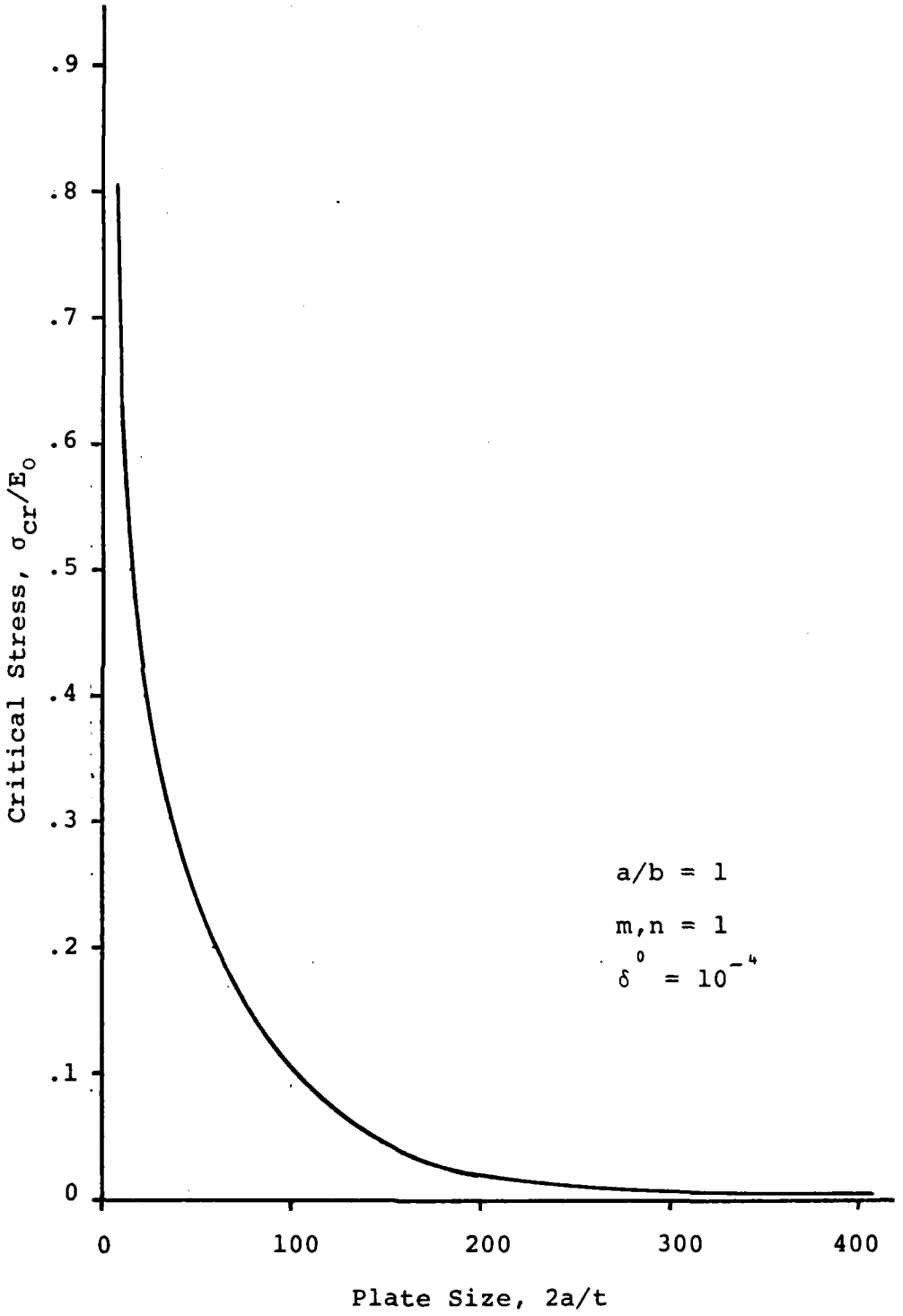

Fig. 4. Effect of Plate Size on Critical Stress for Elastic-Plastic Plate

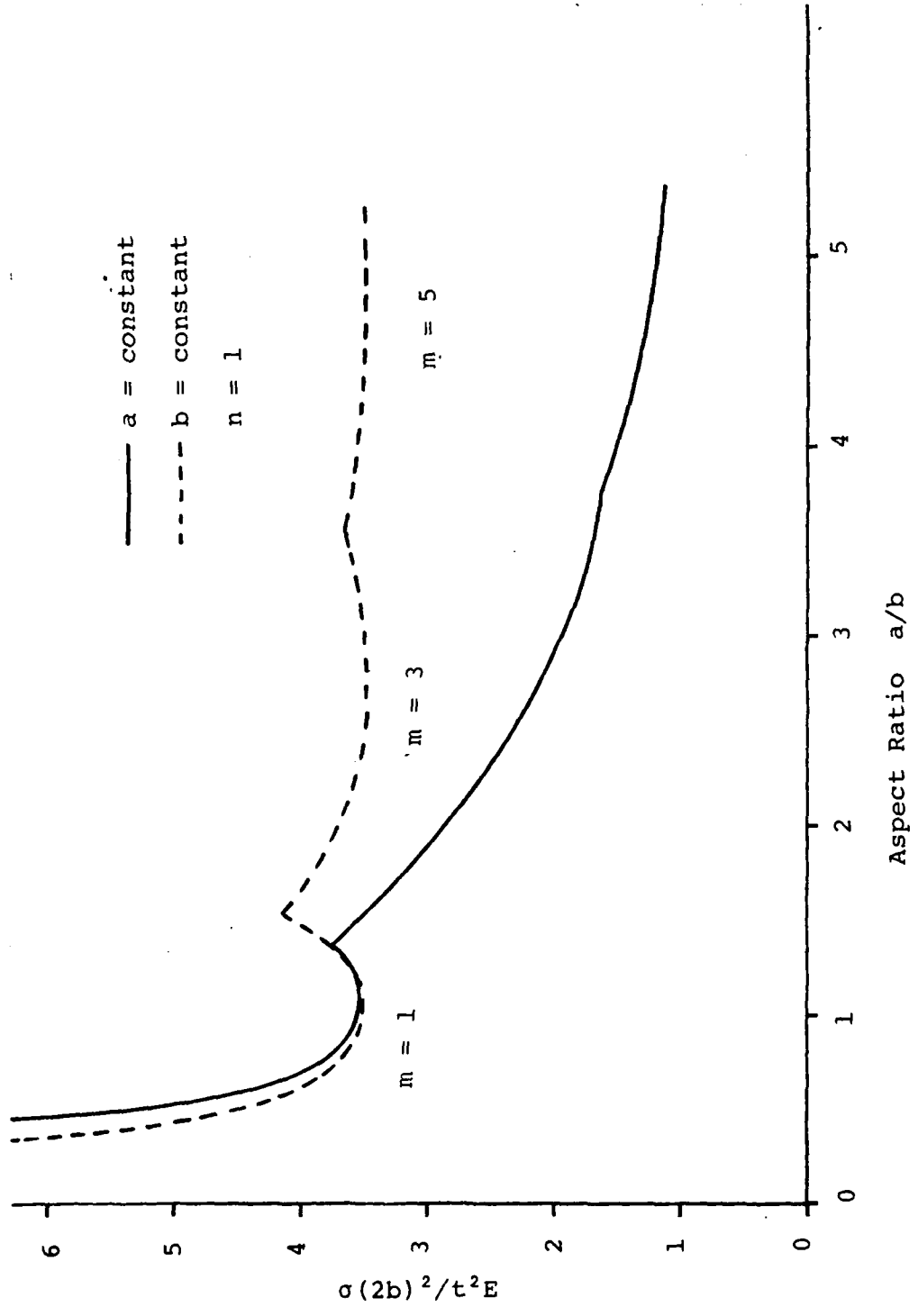

Fig. 5. Effect of Method used to Change a/b Ratio

aspect ratio plotted against the normalized critical stress. It should be noted that as a/b increases the critical stress is minimized at increasing values of m. For a/b less than approximately 1 the critical stress is lower when the width 2b is constant, whereas for a/b greater than 1 the stress is increasingly lower when the length, 2a, is constant. This difference can be explained by comparing the collapse of an elastic-plastic plate with that of an elastic plate and will be discussed fully in the following section.

Elastic Material

Figure 6 shows the stress versus displacement curve for an elastic plate of dimension similar to those of the elastic-plastic plate in Figure 3. The significant difference lies in the fact that the three curves for initial imperfections of $\delta^o = 10^{-2}$, 10^{-4}, and 10^{-6} all rise asymtotically to the same value. It can be shown that this value is the classical bifurcation stress described by the following equation (Reference 3):

$$\sigma_{cr} = \frac{k\pi^2 D}{(2b)A} \tag{24}$$

where

$$k = \left(\frac{mb}{a} + \frac{a}{mb}\right)^2 \tag{25}$$

$$D = \frac{Et^3}{12(1-\nu^2)} \tag{26}$$

A = area of load application, 2bt

Since the stress functions assumed for this problem do not permit evaluation of postbuckling stresses, the

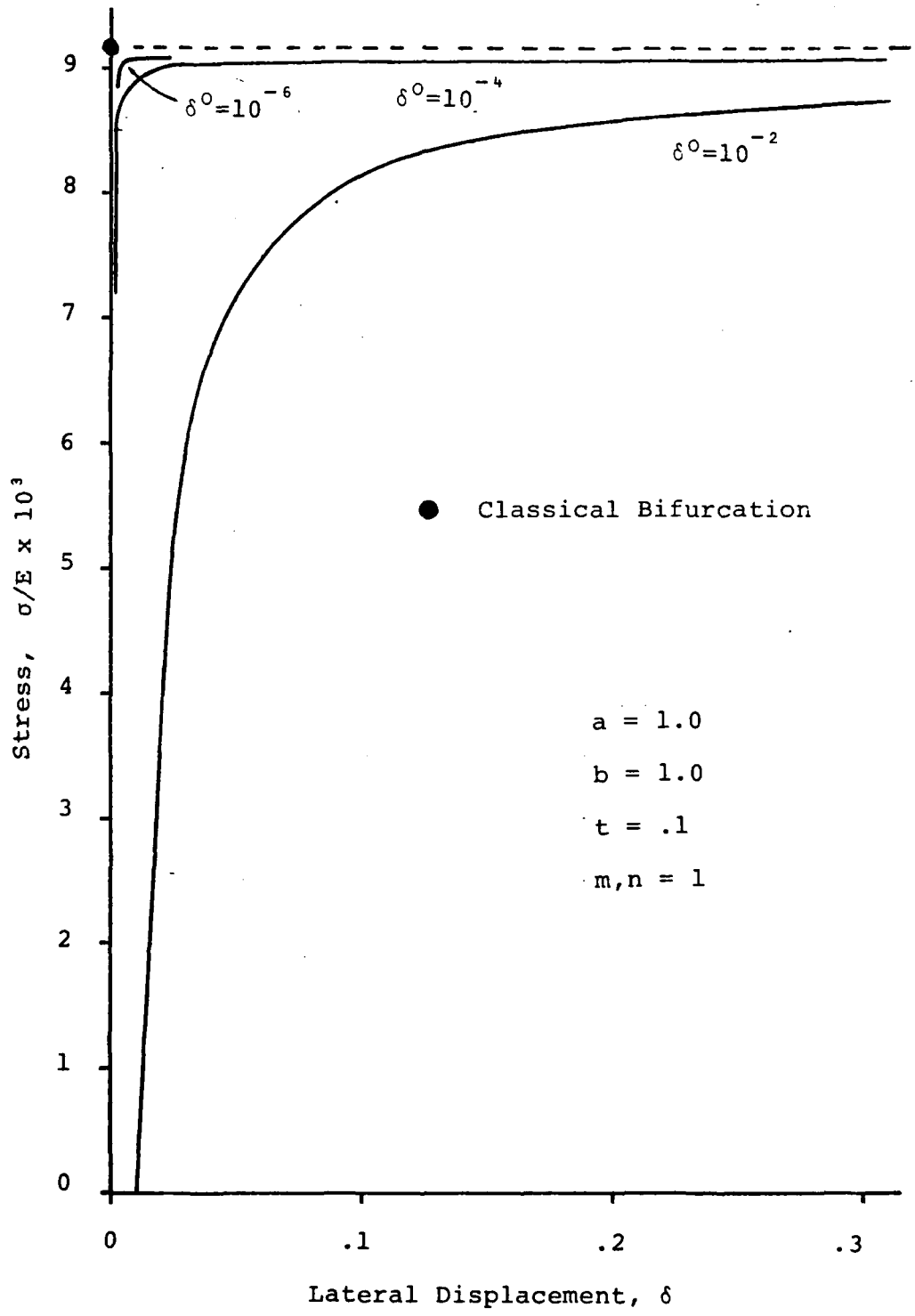

Fig. 6. Stress vs. Displacement for Typical Elastic Material

stress-displacement curve does not rise above the bifurcation stress as would be found in an actual plate. For this reason the stress associated with a lateral displacement of an elastic plate equal to the thickness of the plate is defined as the practical critical stress, σ_{pr}. It is assumed that a deflection beyond this value could be considered as beyond the practical plate limits.

The shape of the load-displacement curves for the different initial imperfections are all similar to those in Figure 6, therefore not all of the curves are shown. In Figure 7, load-displacement curves are shown for two plates of dimension 2a = 5., 2b = 5. and 2a = 10.0, 2b = 10.0, considering an initial imperfection of 10^{-4}. The elastic curves are compared with elastic-plastic curves for the same plates. If, in Figure 7, one compares the critical stresses of the smaller plate with those of the larger plate, it is apparent that the effects of plasticity are significantly more pronounced in the smaller plate than in the larger. In fact, the difference in the large plate is only approximately 7% as compared to approximately 25% for the smaller plate. Comparing the whole spectrum of 2a/t ratios, Figure 8, the effect is obvious. It is clear that in a plate requiring large stress to reach the critical stress, the effects of plasticity are much more pronounced and that in a plate requiring small stress to reach critical limits the plasticity effects become almost negligible. In other words, the thicker

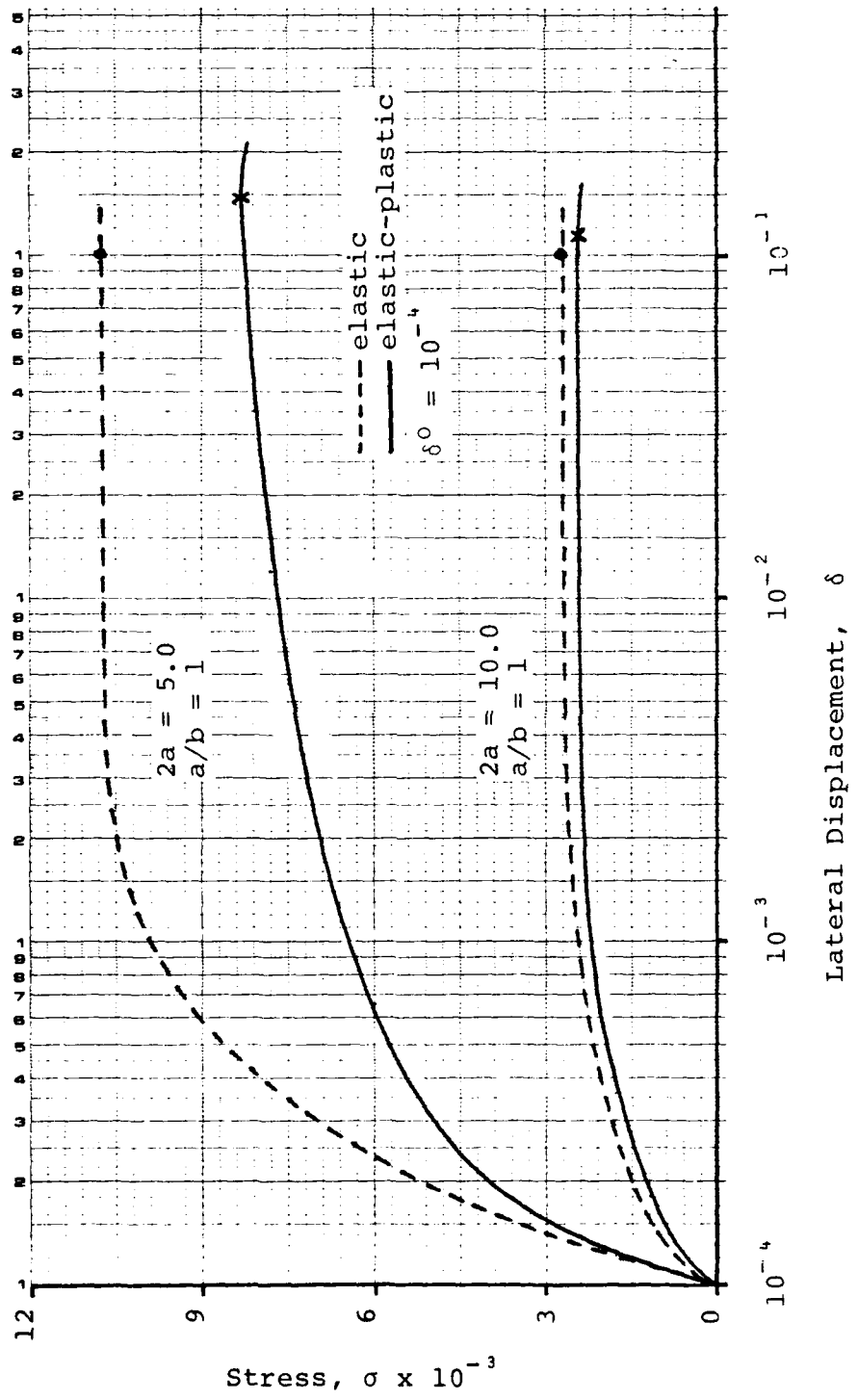

Fig. 7. Load-Displacement Difference Between Plates of Different Size

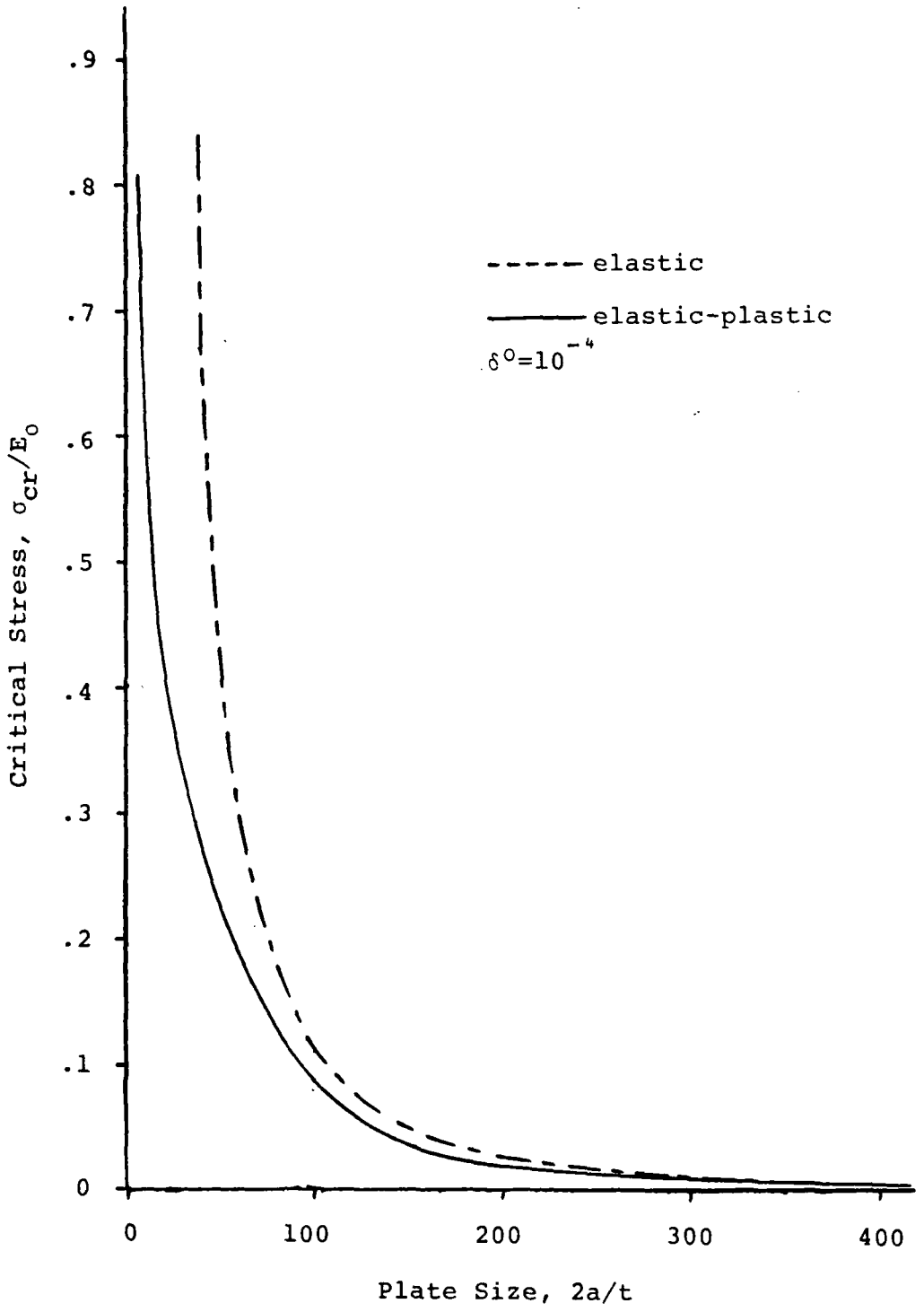

Fig. 8. Comparison of Elastic and Elastic-Plastic Critical Stresses as a Function of Plate Size

the plate the greater the plasticity effects. This can be seen by examining the stress-strain curves for an elastic and elastic-plastic material, Figure 9.

As with the elastic-plastic plates, the effect of changing the a/b ratio was computed for elastic plates. The results are shown in Figure 10 along with the elastic-plastic results. It was found that for an elastic material, it did not make a difference which dimension, a or b, was kept constant and that in fact the same curve was found for both cases.

To explain the fact that the method of changing the a/b ratio affected the outcome in the elastic-plastic case and not in the elastic case, one must look at the effect of the *m* and *n* values. By changing the shape of the imperfection from 1 half-sine to 3 half-sines and, likewise, 5 half-sines, the effect is that it determines the collapse mode, that is, the final shape of the plate. It can be seen from Figure 10, that as the a/b ratio increases the minimum stress for collapse occurs at higher m values and that for an elastic material the mimimum values become asymtotic to some mimimum value. From this, it can be seen that a plate with an initial imperfection of 1 half-sine wave will collapse at the same stress as a plate whose dimensions are odd integers larger than the single half-sine plate, provided an imperfection exists of the same odd integer shape. For example, in the case of a square plate 15 inches by 15 inches with an initial imperfection of 3

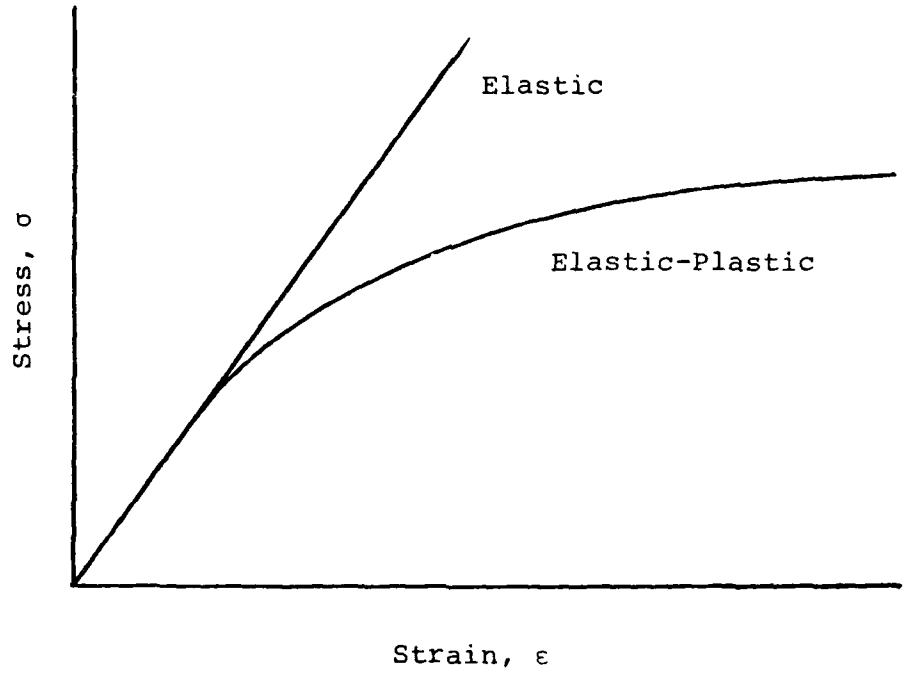

Fig. 9. Stress-Strain Relation for Elastic and Elastic-Plastic Material

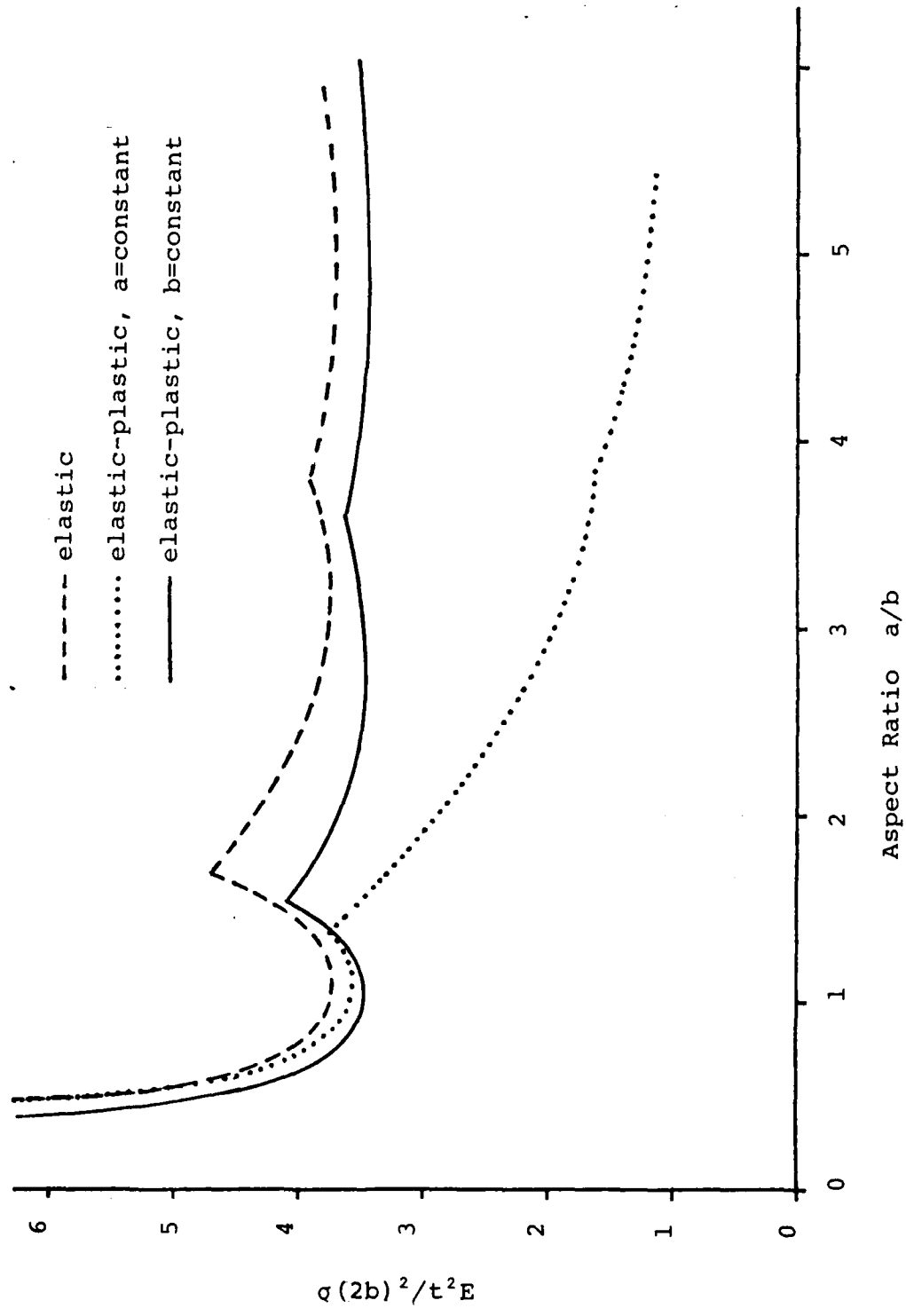

Fig. 10. Comparison of Effect of Changing a/b Ratio

half-sine waves in the x and y directions, the collapse stress is the same as a plate 5 inches by 5 inches, with 1 half-sine imperfection in the x and y direction. Consequently a plate with 1 half-sine wave in each direction can be thought of as an "elemental component" for larger plates. (See Figure 11).

With this concept in mind, one can justify the difference in the two methods of changing the a/b ratio for an elastic-plastic plate. Figure 12 illustrates the variation in a/b using both the constant a and constant b methods. In the b = constant case, for a/b = 3, Figure 12f, the plate is three times as long as the a/b = 1 case, Figure 12e, the minimum collapse stress is found when an initial imperfection of m = 3 is used. Consequently, the "elemental component" is the same size as the a/b = 1 plate and, therefore, the critical stress is the same as the a/b = 1 case. Similar conditions apply for m = 5. For the other method, (a = constant), when a/b = 3, Figure 12c, the size of the "elemental component" is 1/3 as large as the a/b = 1 condition, Figure 12b, and as was shown in Figure 8, as 2 a/t decreases, the plasticity effects become more pronounced. Therefore, the curve for the elastic-plastic with a = constant, Figure 10, is expected to decrease as a/b increases. In effect, the results indicate that a plate, whether elastic or elastic-plastic, with initial imperfections in the x and/or y direction will collapse at the same stress as the "elemental component", that is, the

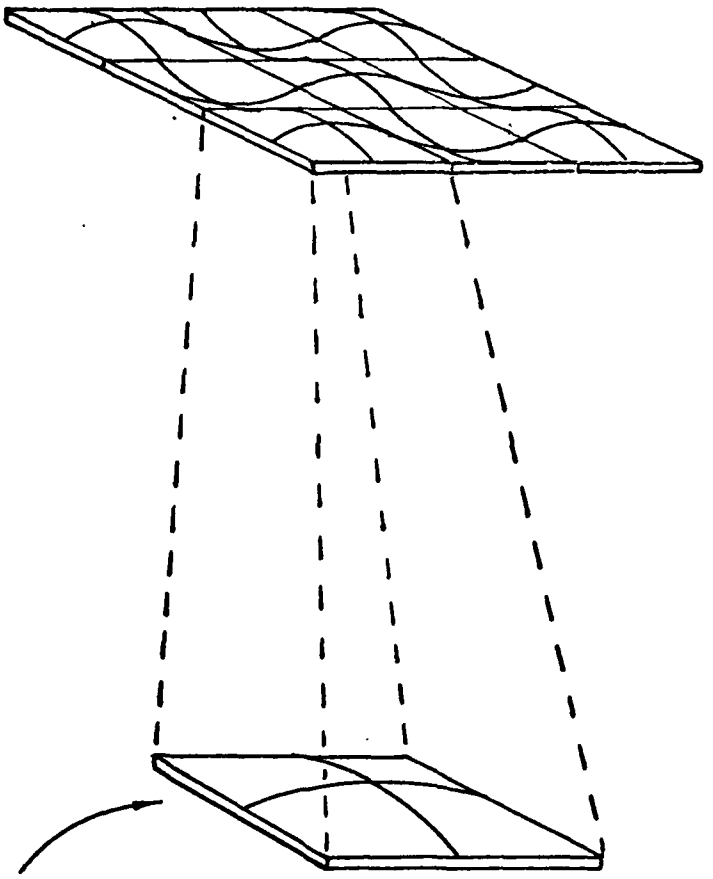

Fig. 11. Elemental Component of Plate with m,n = 3

a = constant

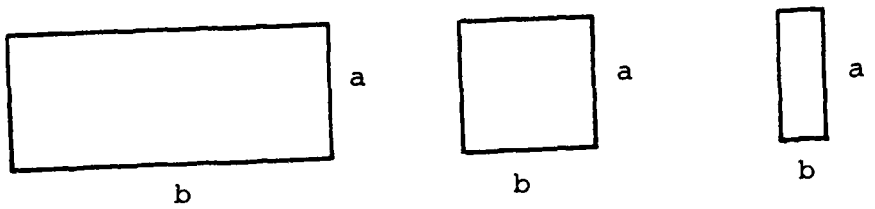

a/b < 1 a/b = 1 a/b > 1

a. b. c.

b = constant

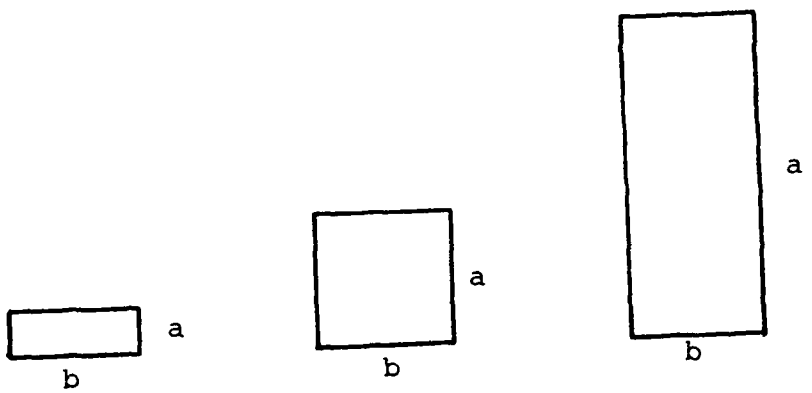

a/b < 1 a/b = 1 a/b > 1

d. e. f.

Fig. 12. Methods of Changing a/b Ratio

integral part of the plate with a single half-sine wave in the x and y direction.

Orthotropic Materials

The orthotropic plate considered in this thesis possesses elastic properties along the major material axis. Consequently, the results found are similar to those of the previous section. A significant interest was in the effect that the orientation of the material had on the critical stress. The material properties are considered to be similar to those of boron-epoxy composite with $E_1/E_2 = 10$, $G_{12}/E_1 = .03$, $\nu_{12} = .3$.

It was determined early in the study that results for off axis orientation were significantly lower than expected. The reason for this can be seen if one examines the differential equation governing an orthotropic plate of arbitrary orientation (11)

$$D_{11}\delta w,_{xxxx} + 4\ D_{16}\delta w,_{xxxy} + 2\ (D_{12} + 2D_{66})\delta w,_{xxyy}$$

$$+ 4D_{26}\ \delta w,_{xyyy} + D_{22}\ \delta w,_{yyyy} + \bar{N}_x\ \delta w,_{xx}$$

where the subscripts denote differentiation with respect to the x and y directions. The bending stiffnesses, D_{ij}, are described in detail in Jones (11). The major difference between this differential equation and that for an orthotropic plate oriented at 0^o and 90^o to the major material

axes, referred to as specially orthotropic, is in the inclusion of the twist coupling stiffnesses, D_{16} and D_{26}. It can be shown that D_{16} and D_{26} are dependent upon the constitutive coefficients C_{13} and C_{23} of Eq. (4). However, the form of the stress function assumed, is such that these cross coupling terms do not carry through the integration and variation of the functional, illustrated in Appendix B. Consequently, the stresses at an orientation other than 0^{o} and 90^{o} are reduced by an amount equivalent to the cross coupling terms. For an orientation of 0^{o} and 90^{o} these terms D_{16} and D_{26}, are not found in the differential equation and consequently reliable results are expected.

Mandell (15) made an experimental investigation on the buckling of anisotropic fiber reinforced plates with boundary conditions similar to those imposed in this report. A boron-epoxy plate 11 inches by 9.75 inches by .096 inches thick, simply-supported along all edges with an in-plane displacement allowed in the normal direction and loaded at $\theta = 0^{o}$, was considered. Results are shown in Figure 13. Comparison is made with curves obtained using an initial imperfection of 10^{-2} and 10^{-3}. Note that the two curves provide upper and lower bounds to the experimental results. This indicates that the inclusion of geometric imperfections does indeed result in load-deflection curves which are representative of actual plates,

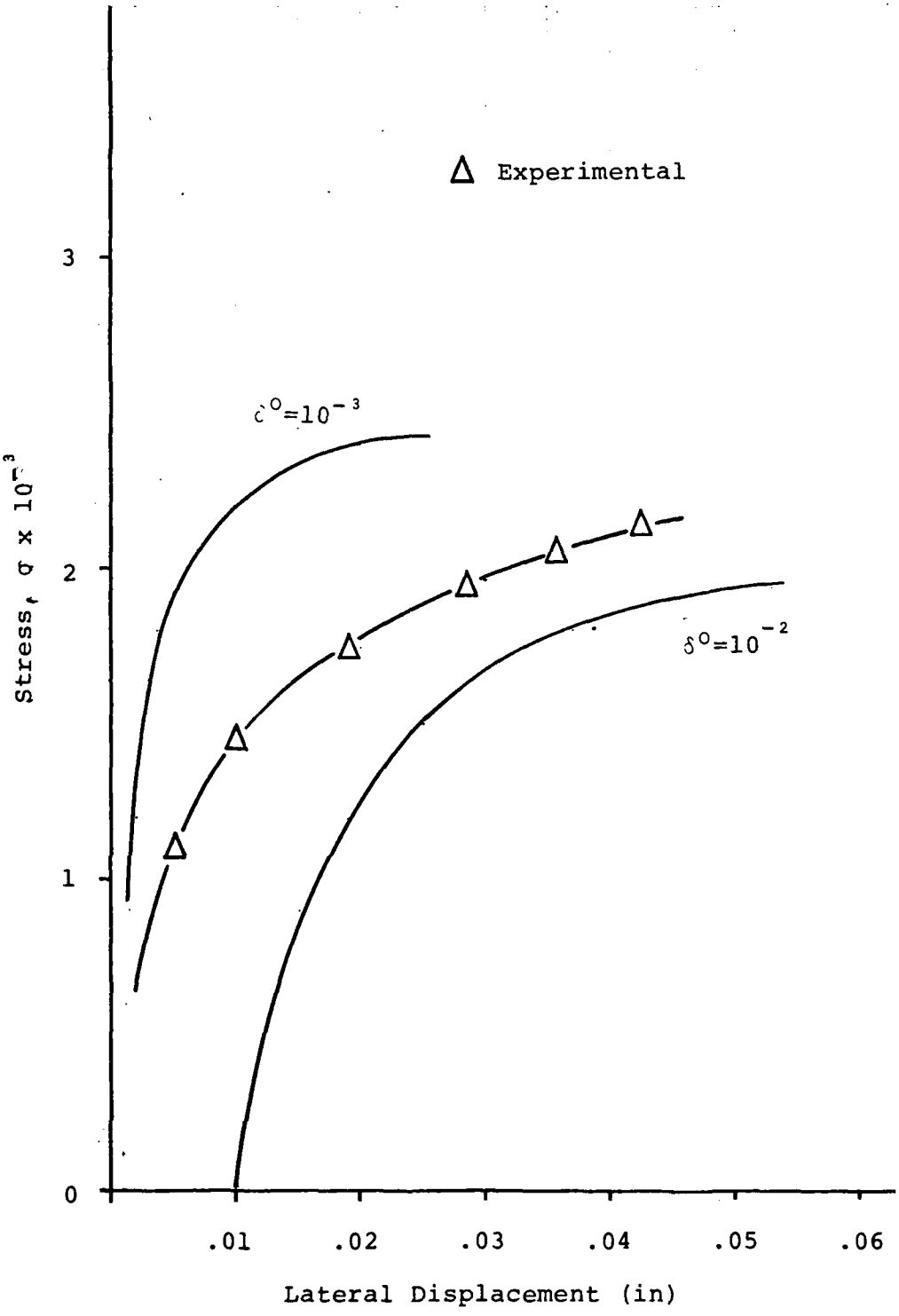

Fig. 13. Comparison of Experimental with Analytical Results for Orthotropic Plate

at least in the initial stages of deflection. The critical stresses are shown for $\theta = 0^{o}$ and 90^{o} along with experimental values for other angles in Figure 14. A Rayleigh-Ritz theoretical solution is also shown. The thesis results compare favorably at $\theta = 0^{o}$. At $\theta = 90^{o}$ the results are considerably above experimental values and even more above the Rayleigh-Ritz solution. The classical buckling mode for this condition is with m = 2; however, the initial imperfection shape, in this case m = 3, establishes the mode at collapse and consequently the critical stress obtained at 90^{o} is higher than the classical value.

For an a/b ratio of 1, the affect of 2a/t is shown on Figure 15. For this case both the $\theta = 0^{o}$ and the $\theta = 90^{o}$ curves are coincident. It can be seen in Figure 16 that this is not necessarily true for other values of a/b. In fact, for a/b less than 1 the critical stress for $\theta = 90^{o}$ becomes significantly less than the $\theta = 0^{o}$ orientation. In Figure 16 the E_1/E_2 ratio is 10, indicating that the strength in the 2-direction is much less than in the 1-direction. If one decreases this ratio, as with a boron/aluminum composite, $E_1/E_2 = 1.44$, the difference between $\theta = 0^{o}$ and 90^{o} becomes less pronounced. (See Figure 17.) This is as expected since as E_1/E_2 tends to 1, essentially isotropic, the curves would merge into one. The results found for the boron/aluminum composite compare very well with results published by Chamis (14) for a/b less than 1. For a/b values greater

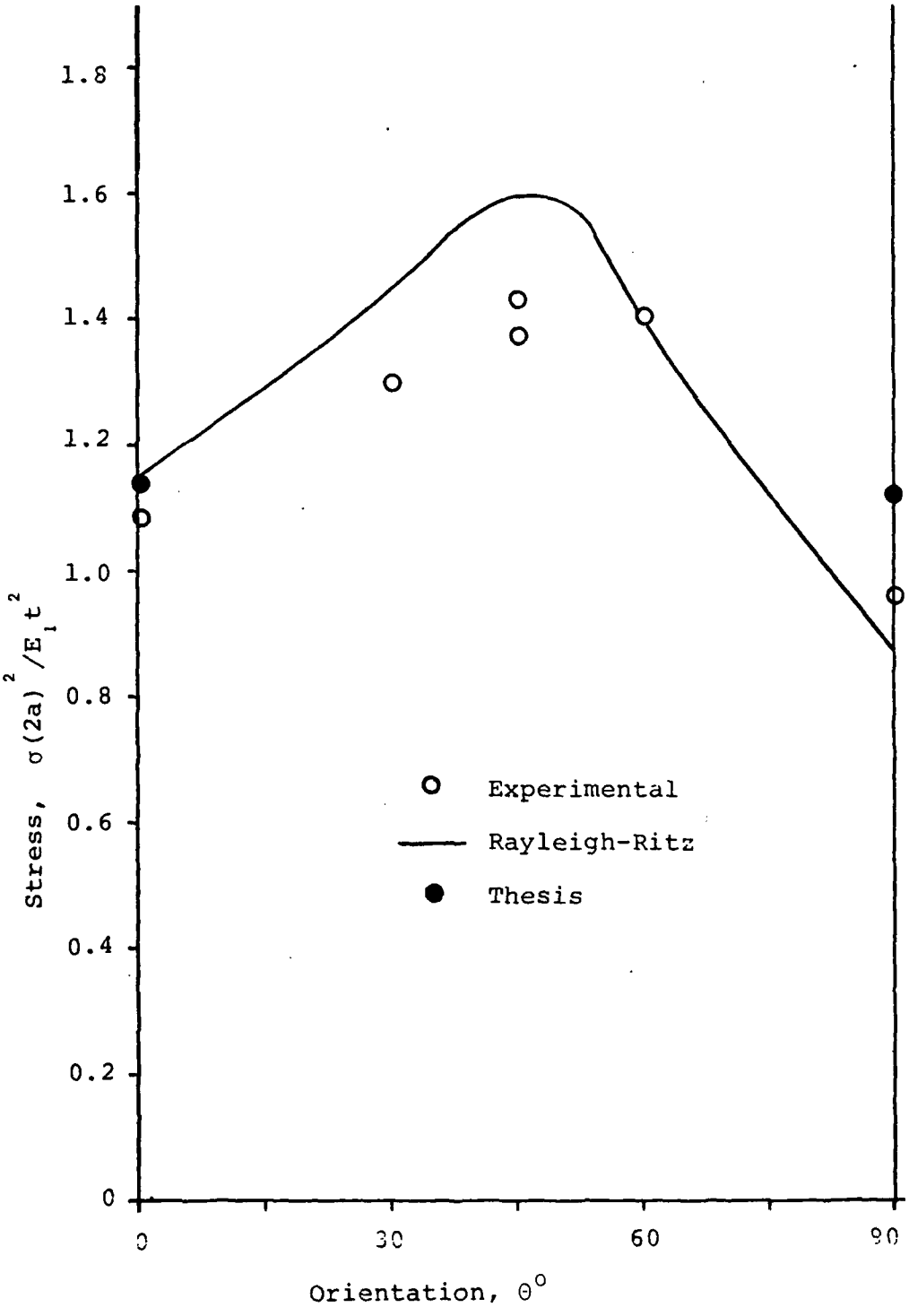

Fig.14 Comparison of Orthotropic Results

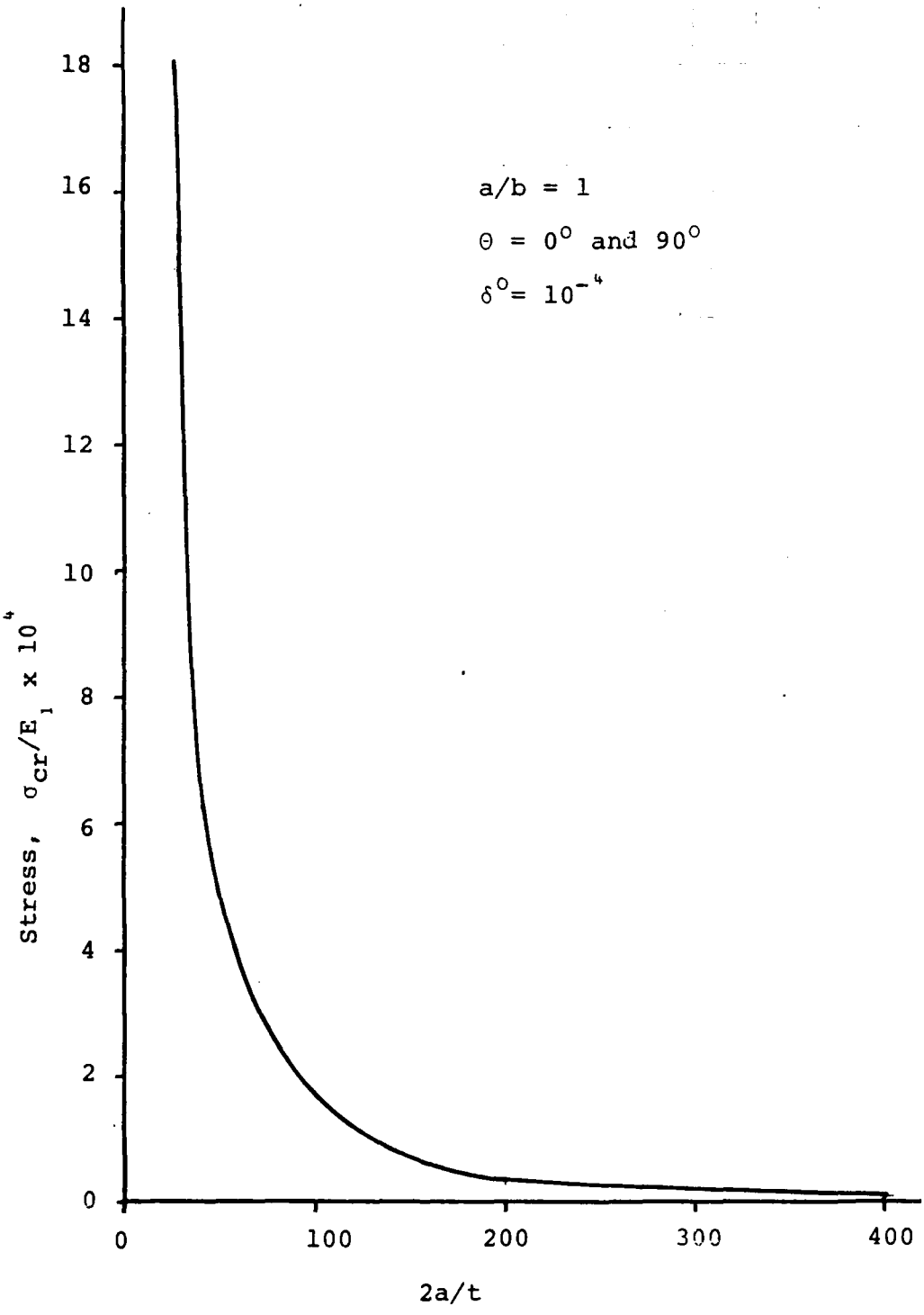

Fig. 15. Affect of 2a/t for $\Theta = 0^{\circ}, 90^{\circ}$

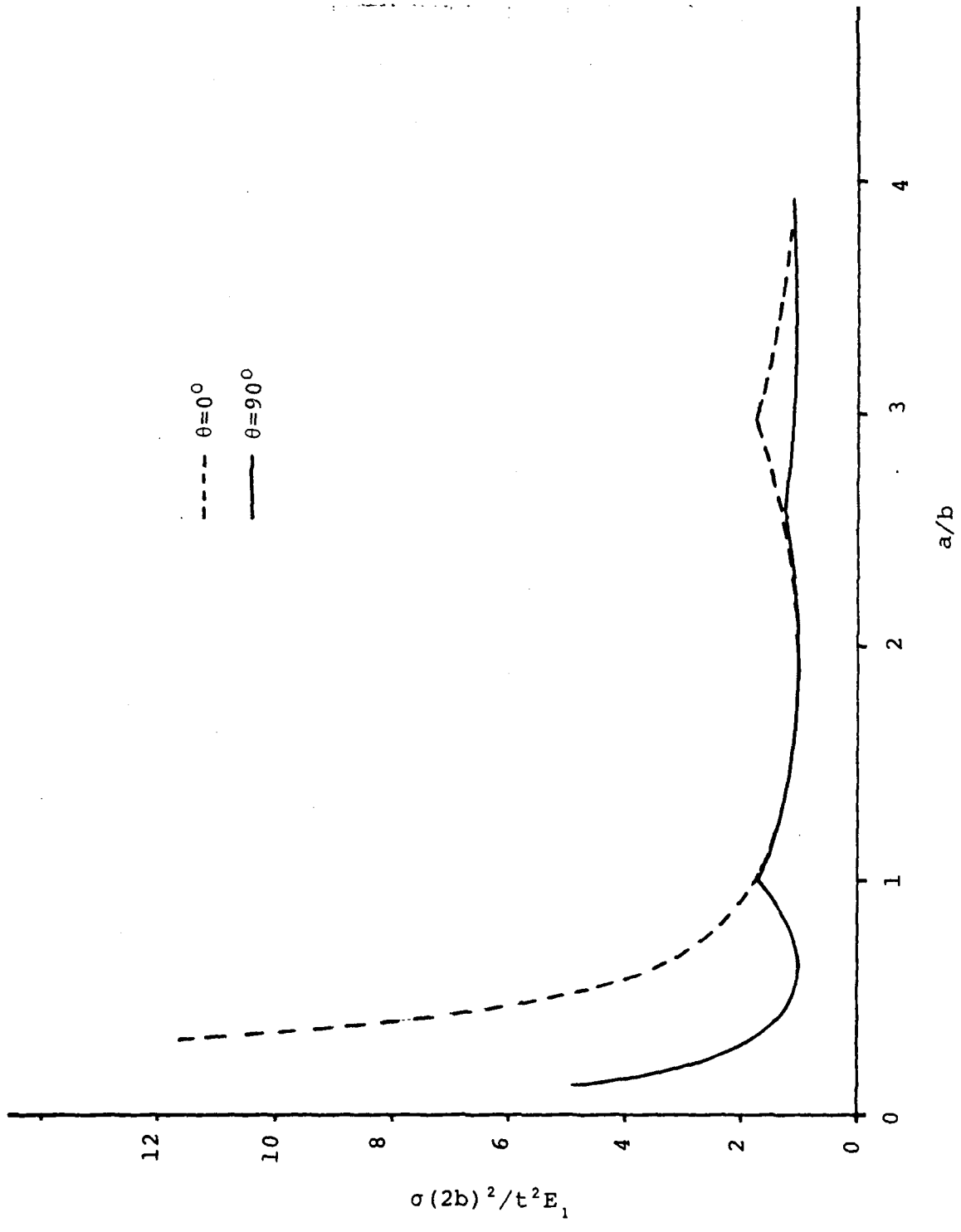

Fig. 16. Comparison of 0° and 90° for Orthotropic Ply

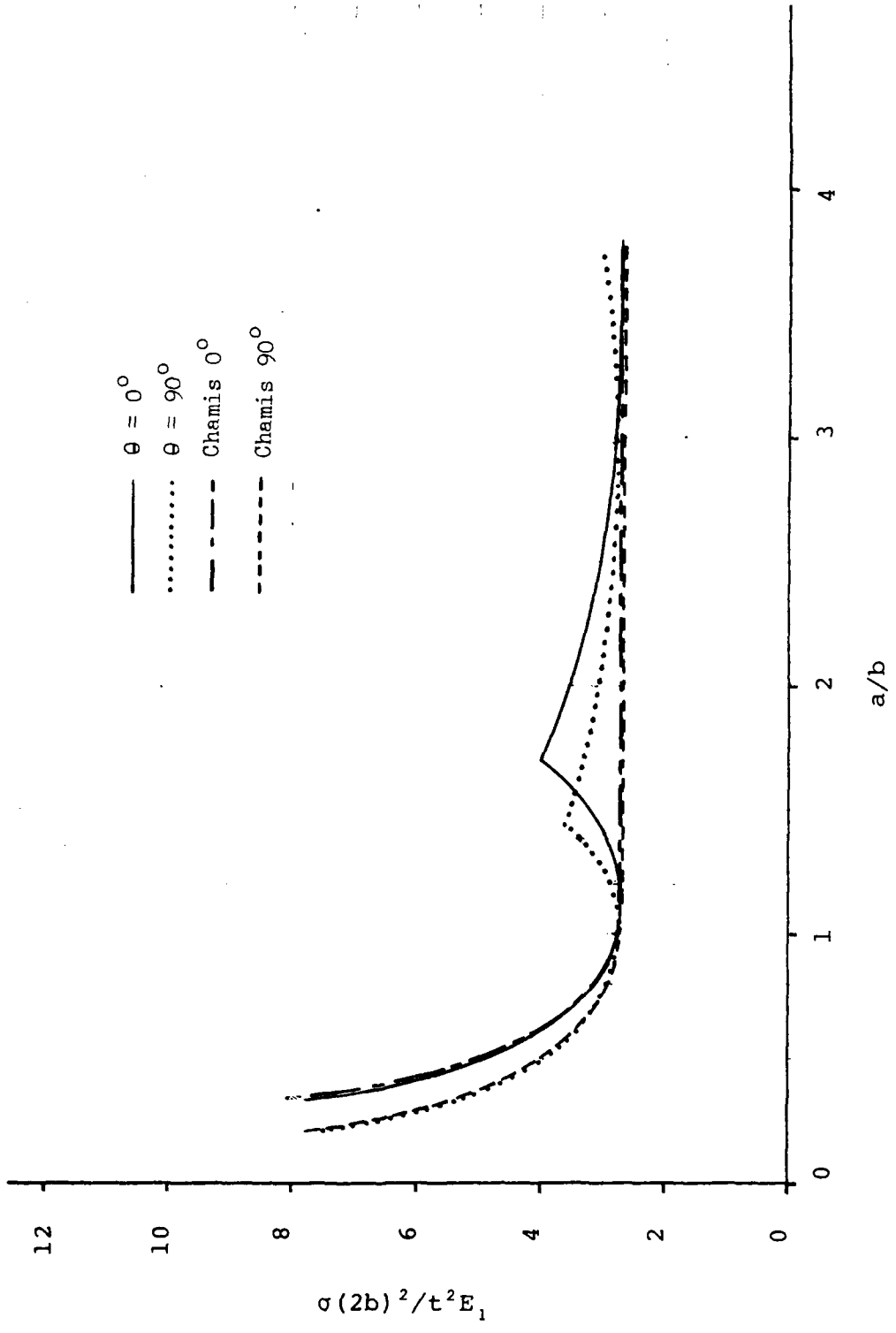

Fig. 17. Affect of a/b Ratio on Boron/Aluminum Plate

than 1, the effect of the imperfection shape, m, is more pronounced but approaches the same minimum stress as published by Chamis as a/b increases.

IV. Conclusions

A. Elastic-Plastic

1. The size of an imperfection greatly affects the load displacement curve. For an elastic-plastic material, not only the degree of displacement at any instant, but the stress at which collapse occurs is dependent upon the imperfection. A plate with a large initial imperfection will collapse at a lower stress and larger displacement than a similar plate with small initial imperfections.

2. As the aspect ratio increases, the normalized stress for a particular m value decreases to a minimum and then begins to increase again. The minimum stress required for collapse is found at increasing values of m for increasing a/b ratios. In all cases the minimum stress is fou... with n = 1.

3. The shape of the initial imperfections determined the shape of the plate at collapse. That is, if a plate has an initial imperfection of m half-sines in the x direction and n half-sines in the y direction, it will collapse in that mode, regardless of plate size or aspect ratio.

4. Plasticity affects become more and more significant as the effective thickness of the plate increases.

5. A plate with an initial imperfection of m, n = 1 is the elemental component from which the critical stress of plates with other imperfection modes may be determined.

B. Elastic

1. The affect of imperfection size is similar to the elastic-plastic material except that the collapse stress becomes asymtotic to the classical bifurcation stress. Because of the form of the assumed stress functions, no postbuckling stresses can be obtained. Consequently, the stress at a displacement equal to the thickness of the plate was assumed to be the practical critical stress.

2. The effect of the magnitude of the imperfection on the practical critical stress becomes more pronounced as the imperfection size increases, that is, the practical critical stress decreases with increasing imperfection size.

3. Critical values computed are dependent upon the imperfection shape, m. Individual critical stresses may be higher than classical values because not all mode shapes are considered.

4. The effects of plate size, aspect ratio and imperfection shape are all similar to those of the elastic-plastic case.

C. Orthotropic

1. Imperfection size and shape, plate size and aspect ratio all have affects similar to those of an elastic isotropic material.

2. The orientation of the plate has a significant effect on the collapse stress at a/b ratios less than 1. The relative difference between E_1 and E_2 determines the magnitude of the difference.

Bibliography

1. Euler, Leonard, Elastic Curves, transulated and annotated by W. A. Oldfather, C A. Ellis, and D. M. Brown, 1933.

2. Bryan, G. H. "On the Stability of the Plane and Plate, with Applications to the "Buckling" of the sides of a Ship." Proc. London Math Soc., Vol 22, pg 54-67, Dec. 11, 1890.

3. Timoshenko, S., Theory of Elastic Stability, First Ed., McGraw Hill, 1946

4. Hill, H. N., "Chart for Critical Compressive Stress of Flat Rectangular Plates", NACA TN 773, 1940.

5. Lundquist, Eugene E., and Stowell, Elbridge, Z., "Critical Compressive Stress for Flat Rectangular Plates Supported Along All Edges and Elastically Restrained Against Rotations Along the Unloaded Edges", NACA Rep. 773, 1942.

6. Onat, E. T., and Drucker, D. C., "Inelastic Instability and Inoremental Theories of Plasticity", Journal of the Aerospace Sciences, Vol 20, pg 181-186, 1953

7. Drucker, D. C., and Onat, E. T., "On the Concept of Stability of Inelastic Systems", Journal of the Aerospace Sciences, Vol 21, pg 543-548, 1954.

8. Neale, K. W., "A Method for the Estimation of Plastic Buckling Loads", International Journal of Solids and Structures, Vol 10, pg 217-230, 1974.

9. Neale, K. W., "Effect of Imperfections on the Plastic Buckling of Rectangular Plates", Journal of Applied Mechanics, March 1975

10. Ashton, J. E., and Whitney, J. M., Theory of Laminated Plates, Technomic Publishing Company, Inc., 1970

11. Jones, R. M., Mechanics of Composite Materials, McGraw Hill, 1975.

12. Chamis, C. C., Composite Materials, Vol 8, Academic Press, 1975.

13. Neale, K. W., "A General Variational Theorem for the Rate Problem in Elastic-Plasticity", International Journal of Solids and Structures, Vol 8, pg 865-876, 1922.

14. Chamis, C. C., "Theoretical Buckling Loads of Boron/Aluminum and Graphite/Resin Fiber-Composite Anisotropic Plates", NASA TN D-6572, 1971-72.

15. Mandell, J. F., "Experimental Investigation of the Buckling of Anisotropic Fiber Reinforced Plastic Plates", AFML-TR-68-281, October, 1968.

16. Reissner, E., "On a Variational Theorem in Elasticity", J. Math Phys. 32, 129 (1953).

17. Reissner, E., "On Variational Theorem for Finite Deformations", J. Math Phys. 32, 129 (1953).

18. Reissner, E., "On Variational Principles in Elasticity, Proc. Symp. Appl. Math. 8, 1 (1958).

19. Reissner, E., "On Some Variational Theorems in Elasticity," Problems of Continuum Mechanics, SIAM, Philadelphia, p. 370 (1961).

20. Fung, Y. C., Foundations of Solid Mechanics, Prentice-Hall, 1965.

21. Murphy, L. M., and Lee, L. H. N., "Inelastic Buckling Process of Axially Compressed Cylindrical Shells Subject to Edge Constraints", International Journal of Solids and Structures, 7, 1153 (1971).

22. Saada, A. S., Elasticity, Pergamon Press Inc., 1974.

Appendix A

Material Properties

1) Elastic Plastic

$E = 30 \times 10^6$ lb/in^2

$E_o = 100{,}000$ lb/in^2

$G = 27/4E_o^3$

$\nu = 0.3$

$k = 3$

2) Elastic

$E = 30 \times 10^6$ lb/in^2

$\nu = 0.3$

3) Orthotropic

Boron-Epoxy

$E_1 = 30 \times 10^6$ lb/in^2

$E_2 = 3.0 \times 10^6$ lb/in^2

$G_{12} = 1.0 \times 10^6$ lb/in^2

$\nu_{12} = 0.3$

Boron-Aluminum

$E_1 = 35 \times 10^6$ lb/in^2

$E_2 = 24.3 \times 10^6$ lb/in^2

$G_{12} = 11.6 \times 10^6$ lb/in^2

$\nu_{12} = 0.24$

Appendix B

Calculation of a_{ij} Matrix

Beginning with the functional,

$$I^{o} = \int_{-t/2}^{t/2} \int_{-b}^{b} \int_{-a}^{a} \left[\dot{\tau}_{ij} \dot{E}_{ij} + \tfrac{1}{2}\tau_{ij} v_{kij} v_{k,j} - W(\dot{\tau}) \right] dxdydz \tag{B1}$$

where $$\dot{\tau}_{ij} \dot{E}_{ij} = \dot{\tau}_{xx} \dot{E}_{xx} + 2\dot{\tau}_{xy} \dot{E}_{xy} + \dot{\tau}_{yy} \dot{E}_{yy} \tag{B2}$$

$$\tau_{ij} v_{k,i} v_{k,j} = \tau_{xx} \left(\frac{\partial \dot{w}}{\partial x}\right)^2 + 2\tau_{xy} \frac{\partial \dot{w}}{\partial x} \frac{\partial \dot{w}}{\partial y} + \tau_{yy} \left(\frac{\partial \dot{w}}{\partial y}\right)^2 \tag{B3}$$

$$2W(\dot{\tau}) = C_{11}\dot{\tau}_{xx}^2 + 2C_{12}\dot{\tau}_{xx}\dot{\tau}_{yy} + C_{22}\dot{\tau}_{yy}^2 + 2C_{13}\dot{\tau}_{xx}\tau_{xy} + 2C_{23}\dot{\tau}_{xy}\dot{\tau}_{yy} + 2C_{33}\dot{\tau}_{xy}^2 \tag{B4}$$

To get I_o in terms of known quantities, substitute the assumed functions

$$\dot{u} = -\dot{\beta}^{*}x \tag{B5a}$$

$$\dot{v} = 0 \tag{B5b}$$

$$\dot{w} = \dot{\delta}t \cos\frac{m\pi x}{2a} \cos\frac{n\pi y}{2b} \tag{B5c}$$

$$\dot{\tau}_{xx} = -\dot{\sigma} + \dot{\alpha}_1 \frac{z}{t} \cos\frac{m\pi x}{2a} \cos\frac{n\pi y}{2b} \tag{B6a}$$

$$\dot{\tau}_{yy} = \dot{\alpha}_2 \frac{z}{t} \cos\frac{m\pi x}{2a} \cos\frac{n\pi y}{2b} \tag{B6b}$$

$$\dot{\tau}_{xy} = \dot{\alpha}_3 \frac{z}{t} \sin\frac{m\pi x}{2a} \sin\frac{n\pi y}{2b} \tag{B6c}$$

$$u = -\beta^{*}x \tag{B7a}$$

$$v = 0 \tag{B7b}$$

$$w = \delta t \cos\frac{m\pi x}{2a} \cos\frac{n\pi y}{2b} \tag{B7c}$$

$$\tau_{xx} = -\sigma + \alpha_1 \frac{z}{t} \cos\frac{m\pi x}{2a} \cos\frac{n\pi y}{2b} \tag{B8a}$$

$$\tau_{yy} = \alpha_2 \frac{z}{t} \cos \frac{m\pi x}{2a} \cos \frac{n\pi y}{2b} \tag{B8b}$$

$$\tau_{xy} = \alpha_3 \frac{z}{t} \sin \frac{m\pi x}{2a} \sin \frac{n\pi y}{2b} \tag{B8c}$$

The strain rate equations are:

$$\dot{E}_{xx} = \frac{\partial \dot{u}}{\partial x} - z \frac{\partial^2 \dot{w}}{\partial x^2} + \frac{\partial w}{\partial x} \frac{\partial \dot{w}}{\partial x} \tag{B9a}$$

$$\dot{E}_{yy} = \frac{\partial \dot{v}}{\partial y} - z \frac{\partial^2 \dot{w}}{\partial y^2} + \frac{\partial w}{\partial y} \frac{\partial \dot{w}}{\partial y} \tag{B9b}$$

$$\dot{E}_{xy} = \tfrac{1}{2} \frac{\partial \dot{u}}{\partial y} + \frac{\partial \dot{v}}{\partial x} - 2z \frac{\partial^2 \dot{w}}{\partial x \partial y} + \frac{\partial w}{\partial x} \frac{\partial \dot{w}}{\partial y} + \frac{\partial \dot{w}}{\partial x} \frac{\partial \dot{w}}{\partial y} \tag{B9c}$$

The derivatives may be found from Equations (B5 - B7),

$$\frac{\partial u}{\partial x} = -\dot{\beta}^*, \quad \frac{\partial \dot{v}}{\partial x} = 0, \quad \frac{\partial \dot{w}}{\partial x} = \frac{-m\pi}{2a} \dot{\delta} t \sin \frac{m\pi x}{2a} \sin \frac{n\pi y}{2b} \tag{B10}$$

$$\frac{\partial \dot{u}}{\partial y} = 0, \quad \frac{\partial \dot{v}}{\partial y} = 0, \quad \frac{\partial \dot{w}}{\partial y} = \frac{-n\pi}{2b} \dot{\delta} t \cos \frac{m\pi x}{2a} \sin \frac{n\pi y}{2b} \tag{B11}$$

$$\frac{\partial^2 \dot{w}}{\partial x^2} = 0 \frac{-m^2\pi^2}{4a^2} \dot{\delta} t \cos \frac{m\pi x}{2a} \cos \frac{n\pi y}{2b} \tag{B12}$$

$$\frac{\partial^2 \dot{w}}{\partial y^2} = \frac{-n^2\pi^2}{4b^2} \dot{\delta} t \cos \frac{m\pi x}{2a} \cos \frac{n\pi y}{2b} \tag{B13}$$

$$\frac{\partial^2 \dot{w}}{\partial x \partial y} = \frac{mn\pi^2}{4ab} \dot{\delta} t \sin \frac{m\pi x}{2a} \sin \frac{n\pi y}{2b} \tag{B14}$$

$$\frac{\partial w}{\partial x} = \frac{-m\pi}{2a} \delta t \sin \frac{m\pi x}{2a} \cos \frac{n\pi y}{2b} \tag{B15}$$

$$\frac{\partial w}{\partial y} = \frac{-n\pi}{2b} \delta t \cos \frac{m\pi x}{2a} \sin \frac{n\pi y}{2b} \tag{B16}$$

If Equations (B10 - 16) are substituted into (B9), the results become

$$\dot{E}_{xx} = -\dot{\beta}^* - z \frac{-m^2\pi^2}{4a^2} \dot{\delta} t \cos \frac{m\pi x}{2a} \cos \frac{n\pi y}{2b}$$

$$+\left(\frac{-m\pi}{2a}\,\delta\, t \sin\frac{m\pi x}{2a}\cos\frac{n\pi y}{2b}\right)\left(\frac{-m\pi}{2a}\,\dot{\delta}\, t \sin\frac{m\pi x}{2a}\cos\frac{n\pi y}{2b}\right)\Bigg] \quad \text{(B17a)}$$

$$\dot{E}_{yy} = \Bigg[-z\left(\frac{-n^2\pi^2}{4b^2}\,\dot{\delta}\, t \cos\frac{m\pi x}{2a}\cos\frac{n\pi y}{2b}\right)$$

$$+\left(\frac{-n\pi}{2b}\,\delta\, t \cos\frac{m\pi x}{2a}\sin\frac{n\pi y}{2b}\right)\left(\frac{-n\pi}{2b}\,\dot{\delta}\, t \cos\frac{m\pi x}{2a}\sin\frac{n\pi y}{2b}\right)\Bigg] \quad \text{(B17b)}$$

$$\dot{E}_{xy} = \tfrac{1}{2}\Bigg[-2z\left(\frac{mn\pi^2}{4ab}\,\dot{\delta}\, t \sin\frac{m\pi x}{2a}\sin\frac{n\pi y}{2b}\right)$$

$$+\left(\frac{-m\pi}{2a}\,\delta\, t \sin\frac{m\pi x}{2a}\cos\frac{n\pi y}{2b}\right)\left(\frac{-n\pi}{2b}\,\dot{\delta}\, t \cos\frac{m\pi x}{2a}\sin\frac{n\pi y}{2b}\right)$$

$$+\left(\frac{-m\pi}{2a}\,\dot{\delta}\, t \sin\frac{m\pi x}{2a}\cos\frac{n\pi y}{2b}\right)\left(\frac{-n\pi}{2b}\,\delta\, t \cos\frac{m\pi x}{2a}\sin\frac{n\pi y}{2b}\right)\Bigg] \quad \text{(B17c)}$$

Equation (B3) can now be rewritten with the use of equations (B8) and (B10 - 16).

$$\tau_{ij}\, v_{k,i}\, v_{k,j} = \Bigg[\left(-\sigma + \alpha_1\,\frac{z}{t}\cos\frac{m\pi x}{2a}\cos\frac{n\pi y}{2b}\right)$$

$$\cdot\left(\frac{-m\pi}{2a}\,\dot{\delta}\, t \sin\frac{m\pi x}{2a}\cos\frac{n\pi y}{2b}\right)\left(\frac{-m\pi}{2a}\,\dot{\delta}\, t \sin\frac{m\pi x}{2a}\cos\frac{n\pi y}{2b}\right)$$

$$+ 2\left(\alpha_3\,\frac{z}{t}\sin\frac{m\pi x}{2a}\sin\frac{n\pi y}{2b}\right)\left(\frac{-m\pi}{2a}\,\dot{\delta}\, t \sin\frac{m\pi x}{2a}\cos\frac{n\pi y}{2b}\right)$$

$$\cdot\left(\frac{-n\pi}{2b}\,\dot{\delta}\, t \cos\frac{m\pi x}{2a}\sin\frac{n\pi y}{2b}\right)$$

$$+\left(\alpha_2\,\frac{z}{t}\cos\frac{m\pi x}{2a}\cos\frac{n\pi y}{2b}\right)\left(\frac{-n}{2b}\,\dot{\delta}\, t \cos\frac{m\pi x}{2a}\sin\frac{n\pi y}{2b}\right)$$

$$\cdot\left(\frac{-n\pi}{2b}\,\dot{\delta}\, t \cos\frac{m\pi x}{2a}\sin\frac{n\pi y}{2b}\right)\Bigg] \quad \text{(B18)}$$

Similarly, the substitution of Equation (B6, 8) into Equation (B4) results in:

$$W(\dot{\tau}) = \tfrac{1}{2}\Bigg[C_{11}\left(-\dot{\sigma} + \dot{\alpha}_1\,\frac{z}{t}\cos\frac{m\pi x}{2a}\cos\frac{n\pi y}{2b}\right)$$

$$\cdot\left(-\dot{\sigma} + \dot{\alpha}_1\,\frac{z}{t}\cos\frac{m\pi x}{2a}\cos\frac{n\pi y}{2b}\right)$$

$$+ 2C_{12}\left(-\dot{\sigma} + \dot{\alpha}_1 \frac{z}{t} \cos \frac{m\pi x}{2a} \cos \frac{n\pi y}{2b}\right)\left(\dot{\alpha}_2 \frac{z}{t} \cos \frac{m\pi x}{2a} \cos \frac{n\pi y}{2b}\right)$$

$$+ C_{22}\left(\dot{\alpha}_2 \frac{z}{t} \cos \frac{m\pi x}{2a} \cos \frac{n\pi y}{2b}\right)\left(\dot{\alpha}_2 \frac{z}{t} \cos \frac{m\pi x}{2a} \cos \frac{n\pi y}{2b}\right)$$

$$+ 2C_{13}\left(-\dot{\sigma} + \dot{\alpha}_1 \frac{z}{t} \cos \frac{m\pi x}{2a} \cos \frac{n\pi y}{2b}\right)\left(\dot{\alpha}_3 \frac{z}{t} \sin \frac{m\pi x}{2a} \sin \frac{n\pi y}{2b}\right)$$

$$+ 2C_{23}\left(\dot{\alpha}_3 \frac{z}{t} \sin \frac{m\pi x}{2a} \sin \frac{n\pi y}{2b}\right)\left(\dot{\alpha}_2 \frac{z}{t} \cos \frac{m\pi x}{2a} \cos \frac{n\pi y}{2b}\right)$$

$$+ 2C_{33}\left(\dot{\alpha}_3 \frac{z}{t} \sin \frac{m\pi x}{2a} \sin \frac{n\pi y}{2b}\right)\left(\dot{\alpha}_3 \frac{z}{t} \sin \frac{m\pi x}{2a} \sin \frac{n\pi y}{2b}\right)\Big] \quad \text{(B19)}$$

The expansion of Equation (B2), using (B6) and (B17), produces

$$\dot{\tau}_{xx}\dot{E}_{xx} = \dot{\sigma}\dot{\beta}^* + \dot{\sigma}z\left(\frac{-m^2\pi^2}{4a^2}\dot{\delta}\, t \cos \frac{m\pi x}{2a} \cos \frac{n\pi y}{2b}\right)$$

$$-\left(\dot{\sigma} \frac{m^2\pi^2 t^2}{4a^2}\dot{\delta}\,\dot{\delta} \sin^2 \frac{m\pi x}{2a} \cos^2 \frac{n\pi y}{2b}\right)$$

$$-\dot{\beta}^*\dot{\alpha}_1 \frac{z}{t} \cos \frac{m\pi x}{2a} \cos \frac{n\pi y}{2b} + \dot{\alpha}_1 \frac{z^2m^2\pi^2}{4a^2}\dot{\delta} \cos^2 \frac{m\pi x}{2a} \cos^2 \frac{n\pi y}{2b}$$

$$+\dot{\alpha}_1 z \frac{m^2\pi^2 t}{4a^2}\dot{\delta}\,\dot{\delta}\left(\cos \frac{m\pi x}{2a} \cos \frac{n\pi y}{2b}\right)\left(\sin^2 \frac{m\pi x}{2a} \cos^2 \frac{n\pi y}{2b}\right) \quad \text{(B20a)}$$

$$2\dot{\tau}_{xy}\dot{E}_{xy} = -2\dot{\alpha}_3 z^2 \dot{\delta} \sin^2 \frac{m\pi x}{2a} \sin^2 \frac{n\pi y}{2b}$$

$$+2 \dot{\alpha}_3 zt \frac{mn\pi^2}{4ab}\dot{\delta}\,\dot{\delta} \sin^2 \frac{m\pi x}{2a} \sin^2 \frac{n\pi y}{2b} \cos \frac{m\pi x}{2a} \cos \frac{n\pi y}{2b} \quad \text{(B20b)}$$

$$\dot{\tau}_{yy}\dot{E}_{yy} = \dot{\alpha}_2 \frac{z^2n^2\pi^2}{4b^2}\dot{\delta} \cos^2 \frac{m\pi x}{2a} \cos^2 \frac{n\pi y}{2b}$$

$$+\dot{\alpha}_2 \frac{zn^2\pi^2 t}{4b^2}\dot{\delta}\,\dot{\delta} \cos^3 \frac{m\pi x}{2a} \cos \frac{n\pi y}{2b} \sin^2 \frac{n\pi y}{2b} \quad \text{(B20c)}$$

Since not all the terms of the integrand of I^o involve all the incremental parameters, it simplifies the mathematics to take the variation of the integrand with respect to $\dot{\delta}$, $\dot{\sigma}$, $\dot{\alpha}_1$, $\dot{\alpha}_2$, $\dot{\alpha}_3$ before performing the integration, with the result that

several of the partial derivatives become zero. Switching the order of the integration and the variation does not affect the solution since the variation is taken with respect to parameters independent of the integration parameters x, y, and z. Consequently,

$$\frac{\partial}{\partial \dot{\delta}} \left[\iiint \left(\dot{\tau}_{ij} \dot{E}_{ij} + \tfrac{1}{2} \tau_{ij} v_{k,i} v_{k,j} - W(\dot{\tau}) \right) dx\, dy\, dz \right]$$

becomes

$$\iiint \left[\frac{\partial}{\partial \dot{\delta}} \left(\dot{\tau}_{ij} \dot{E}_{ij} + \tfrac{1}{2} \tau_{ij} v_{k,i} v_{k,j} - W(\dot{\tau}) \right) \right] dx\, dy\, dz \qquad \text{(B21)}$$

with similar expressions for the remaining incremental parameters. Carrying out the above actions involves considerable algebra and simple calculus and therefore all the required steps are not shown. It should be observed that by assuming a function for stress intensity of the same form as the imperfection, one obtains relations which reduce the complexity of the mathematics. This however, eliminates the possibility of relating the stress boundary to a post buckling consideration. Thus, one of the drawbacks to a stress intensity function along a boundary is to produce what may be thought of as unrealistic displacement conditions. The approach followed herein is an attempt to isolate imperfections and as such the stress expressions assumed, can be justified.

The $W(\dot{\tau})$ term of the functional I^o, contains the constitutive coefficients C_{ij}, that vary with material property. To illustrate, the calculation of a_{23} is shown as an example. From Equation (23) of Section II it can be seen that a_{23} is the coefficient of $\dot{\alpha}_1$ in the variation of I^o with respect to $\dot{\sigma}$. Upon taking the variation of the integrand of I^o with respect to $\dot{\sigma}$, the expressions become:

$$\frac{\partial(\dot{\tau}_{ij}\ E_{ij})}{\partial\dot{\sigma}} = \dot{\beta}^* - z\ \frac{m^2\pi^2}{4a^2}\ \dot{\delta}t\ \cos\frac{m\pi x}{2a}\ \cos\frac{n\pi y}{2b}$$

$$-\frac{m^2\pi^2t^2}{4a^2}\ \delta\ \dot{\delta}\ \sin^2\frac{m\pi x}{2a}\ \cos^2\frac{n\pi y}{2b} \qquad \text{(B22)}$$

$$\frac{\partial(\tau_{ij}\ v_{k,i}\ v_{k,j})}{\partial\dot{\sigma}} = 0$$

$$\frac{\partial\ W(\dot{\tau})}{\partial\dot{\sigma}} = -C_{11}\ \dot{\alpha}_1\ \frac{z}{t}\ \cos\frac{m\pi x}{2a}\ \cos\frac{n\pi y}{2b} \qquad \text{(B23a)}$$

The only term containing a coefficient of $\dot{\alpha}_1$ is Equation (23a), consequently to find a_{23} one must integrate (B23a). However, C_{11} must be expressed in terms of the material constitutive relations. For an elastic-plastic Equation (B23a) is expanded to:

$$\frac{\partial(W(\dot{\tau})}{\partial\dot{\sigma}} = -\Bigg[\frac{1}{E}\ \dot{\alpha}_1\ \frac{z}{t}\ \cos\frac{m\pi x}{2a}\ \cos\frac{n\pi y}{2b}$$

$$+\frac{G}{9}\Big(4\ \sigma^2\ \dot{\alpha}_1\ \cos\frac{m\pi x}{2a}\ \cos\frac{n\pi y}{2b} - 4\ \sigma\ \alpha_1\ \alpha_1\ \frac{z^2}{t^2}\ \cos^2\frac{m\pi x}{2a}$$

$$\cdot\ \cos^2\frac{n\pi y}{2b}$$

$$+2\sigma\alpha_2\dot{\alpha}_1\frac{z^2}{t^2}\cos\frac{m\pi x}{2a}\cos\frac{n\pi y}{2b} - 4\sigma\alpha_1\dot{\alpha}_1\frac{z^2}{t^2}\cos^2$$

$$\frac{m\pi x}{2a}\cos^2\frac{n\pi y}{2b}$$

$$+\dot{\alpha}_1\ 4a_1^2\frac{z^3}{t^3}\cos^3\frac{m\pi x}{2a}\cos^3\frac{n\pi y}{2b} - 2\alpha_1\alpha_2\dot{\alpha}_1\frac{z^3}{t^3}\cos^3\frac{m\pi x}{2a}$$

$$\cos^3\frac{n\pi y}{2b}$$

$$+2\sigma\alpha_2\dot{\alpha}_1\frac{z^2}{t^2}\cos^2\frac{m\pi x}{2a}\cos^2\frac{n\pi y}{2b} - 2\alpha_1\alpha_2\dot{\alpha}_1\frac{z^3}{t^3}\cos^3$$

$$\frac{m\pi x}{2a}\cos^3\frac{n\pi y}{2b}$$

$$+\alpha_1^2\dot{\alpha}_1\frac{z^3}{t^3}\cos^3\frac{m\pi x}{2a}\cos^3\frac{n\pi y}{2b}\Big)\Big] \qquad \text{(B23b)}$$

The above expression is integrated as shown

$$\int_{-t/2}^{t/2}\int_{-b}^{b}\int_{-a}^{a}\frac{\partial\left(W(\tau)\right)}{\partial\dot{\sigma}}\ dxdydz$$

During the integration with respect to z, all terms containing odd powers of z go to zero due to the symmetry of the plate. Consequently, the expression is reduced to:

$$\int_{-t/2}^{t/2}\int_{-b}^{b}\int_{-a}^{a}\Big[\frac{G}{9}\left(8\sigma\alpha_1\dot{\alpha}_1 - 4\sigma\alpha_2\dot{\alpha}_1\right)\frac{z^2}{t}\cos^2\frac{m\pi x}{2a}$$

$$\cdot\cos^2\frac{n\pi y}{2b}\Big]\ dxdydz \qquad \text{(B23c)}$$

Factoring constants outside the integral and integrating with respect to z produces:

$$\frac{Gt}{108}\left(8\,\sigma\alpha_1\dot{\alpha}_1 - 4\,\sigma\alpha_2\dot{\alpha}_1\right)\int_{-b}^{b}\int_{-a}^{a}\left(\cos\ \frac{m\pi x}{2a}\cos\ \frac{n\pi y}{2b}\right)dxdy \qquad (23d)$$

Integrating in x and y, using

$$\int \cos^2 C\lambda\, d\lambda = \frac{\lambda}{2} + \frac{\sin 2C\lambda}{4C}$$

where $\frac{m\pi}{2a} = C$

For odd values of m and n, the expression reduces to:

$$\frac{\partial I^{o}}{\partial\dot{\delta}}\,\dot{\alpha}_i = \frac{1}{27}\,G\sigma\left(2\alpha_1-\alpha_2\right)\dot{\alpha}_1\ \text{(tba)} \qquad (23e)$$

Since the only values of m and n that will fulfill the boundary conditions are odd integers, i.e., 1, 3, 5..., Equation (B23e) is the complete form of the expression. Upon completion of all calculations involving the coefficient of the a_{2j} row, the quantity in parentheses, (tba), may be divided out of the equation, leaving:

$$a_{23} = \frac{1}{27}\,G\sigma\left(2\alpha_1-\alpha_2\right) \qquad (B24)$$

In a similar manner the remaining a_{ij} terms can be found. For an elastic-plastic material, the a_{ij} coefficients are calculated to be:

$$a_{11} = \sigma$$

$$a_{12} = \delta$$

$$a_{13} = -\frac{1}{12}$$

$$a_{14} = -\frac{1}{12}\left(\frac{na}{mb}\right)^2,$$

$$a_{15} = \frac{1}{6}\frac{na}{mb},$$

$$a_{21} = \left(\frac{m\pi t}{2a}\right)^2 \delta,$$

$$a_{22} = \frac{4}{E} + \frac{G}{9}\left[16\,\sigma^2 + \frac{1}{12}\left(2\alpha_1 - \alpha_2\right)^2\right.,$$

$$a_{23} = \frac{G\sigma}{27}\left(2\alpha_1 - \alpha_2\right)$$

$$a_{24} = -\frac{G\sigma}{108}\left(4\alpha_1 - 5\alpha_2\right),$$

$$a_{25} = \frac{G\sigma}{9}\,\alpha_3$$

$$a_{31} = \left(\frac{m\pi t}{2a}\right)^2,$$

$$a_{32} = -\frac{12}{27}\,G\sigma\left(2\alpha_1 - \alpha_2\right),$$

$$a_{33} = -\frac{1}{E} - G\left(\frac{12}{27}\,\sigma^2 + \frac{3}{320}\left(2\alpha_1 - \alpha_2\right)^2\right.,$$

$$a_{34} = \frac{\nu}{E} - G\left[\frac{3}{320}\left(2\alpha_1 - \alpha_2\right)\left(2\alpha_2 - \alpha_1\right) - \frac{2}{9}\,\sigma^2\right]$$

$$a_{35} = -\frac{G}{160}\,\alpha_3\left(2\alpha_1 - \alpha_2\right),$$

$$a_{41} = \left(\frac{n\pi t}{2b}\right)^2$$

$$a_{42} = \frac{G\sigma}{9}\left(4\alpha_1 - 5\alpha_2\right)$$

$$a_{43} = a_{34}$$

$$a_{44} = -\frac{1}{E} - G\left[\frac{1}{9}\,\sigma^2 + \frac{3}{320}\left(2\alpha_2 - \alpha_1\right)^2\right.$$

$$a_{45} = -\frac{G}{160}\,\alpha_3\left(2\alpha_2 - \alpha_1\right)$$

$$a_{51} = \left(\frac{m\pi t}{2a}\right)\left(\frac{n\pi t}{2b}\right),$$

$$a_{52} = \frac{2}{3} G\sigma\alpha_3$$

$$a_{53} = \frac{G}{320} \alpha_3 \left(2\alpha_1 - \alpha_2\right),$$

$$a_{54} = \frac{G}{320} \alpha_3 \left(2\alpha_2 - \alpha_1\right),$$

$$a_{55} = \frac{1+\nu}{E} + \frac{27}{160} G\alpha_3^2 \qquad \text{(B25)}$$

If one applies Equation (B23a) to an elastic material and makes the substitution for C_{11} the calculation simplifies as follows

$$\frac{\partial W(\dot{\tau})}{\partial \dot{\sigma}} = -C_{11} \dot{\alpha}_1 \frac{z}{t} \cos \frac{m\pi x}{2a} \cos \frac{n\pi y}{2b} \qquad \text{(B23a)}$$

where

$$C_{11} = \frac{1}{E}$$

Again, the integral reduces to zero when integrated with respect to z. Consequently,

$$a_{23} = 0$$

Likewise, the remaining a_{ij} coefficients for a material displaying elastic properties are determined as:

$$a_{11} = \sigma, \qquad a_{12} = \delta$$

$$a_{13} = \frac{-1}{12}, \qquad a_{14} = \frac{-1}{12} \left(\frac{na}{mb}\right)^2$$

$$a_{15} = \frac{1}{6}\left(\frac{na}{mb}\right), \qquad a_{21} = \left(\frac{m\pi t}{2a}\right)^2 \delta$$

$$a_{22} = 4\,C_{11} \qquad a_{23} = 0$$

$$a_{24} = 0 \qquad a_{25} = 0$$

$$a_{31} = \left(\frac{m\pi t}{2a}\right)^2 \qquad a_{32} = 0$$

$$a_{33} = -C_{11} \qquad a_{34} = -C_{12}$$

$$a_{35} = 0 \qquad a_{41} = \left(\frac{n\pi t}{2b}\right)^2$$

$$a_{42} = 0 \qquad a_{43} = a_{34}$$

$$a_{44} = -C_{22} \qquad a_{45} = 0$$

$$a_{51} = \left(\frac{m\pi t}{2a}\right)\left(\frac{n\pi t}{2b}\right) \qquad a_{52} = 0$$

$$a_{53} = 0 \qquad a_{54} = 0$$

$$a_{55} = C_{33} \qquad \text{(B26)}$$

where C_{ij} is given by Equation (10) of Section II.

Since the only difference between the elastic and orthotropic constitutive relations are through the inclusion of the differences in properties in the longitudinal and transverse direction, and in the coupling of the properties, very little difference is found in the calculation of the a_{ij} matrix. Consequently, the a_{ij} terms for a material displaying orthotropic properties can be expressed as those found in (B26) where the C_{ij}'s are given by Equation (11) of Section II.

VITA

Lyle G. Peck was born on 29 January 1950 in Newberg, Oregon and graduated from Newberg Union High School in 1968. He attended Oregon State University from which he graduated with a Bachelor of Science Degree in mechanical engineering and a commission through the Air Force Reserve Officer Training Program (AFROTC). He served four years as a minuteman missile launch officer at Malmstrom Air Force Base, Great Falls, Montana. While at Great Falls he completed a Masters Degree in Systems Management through the University of Southern California. Upon completion of his tour of missile duty, he was accepted to the Graduate Aeronautical Engineering School of the Air Force Institute of Technology, Wright Patterson Air Force Base, Ohio, in June 1978.

UNCLASSIFIED

SECURITY CLASSIFICATION OF THIS PAGE *(When Data Entered)*

REPORT DOCUMENTATION PAGE		READ INSTRUCTIONS BEFORE COMPLETING FORM
1. REPORT NUMBER AFIT/GAE/AA/79D-14	2. GOVT ACCESSION NO.	3. RECIPIENT'S CATALOG NUMBER
4. TITLE *(and Subtitle)* EFFECT OF IMPERFECTIONS ON THE COLLAPSE OF RECTANGULAR PLATES USING VARIATIONAL CALCULUS		5. TYPE OF REPORT & PERIOD COVERED MS Thesis 6. PERFORMING ORG. REPORT NUMBER
7. AUTHOR(s) Lyle G. Peck Capt USAF		8. CONTRACT OR GRANT NUMBER(s)
9. PERFORMING ORGANIZATION NAME AND ADDRESS Air Force Institute of Technology (AFIT/EN) Wright-Patterson, AFB, Ohio 45433		10. PROGRAM ELEMENT, PROJECT, TASK AREA & WORK UNIT NUMBERS
11. CONTROLLING OFFICE NAME AND ADDRESS		12. REPORT DATE December 1979 13. NUMBER OF PAGES 72
14. MONITORING AGENCY NAME & ADDRESS*(if different from Controlling Office)*		15. SECURITY CLASS. *(of this report)* UNCLASSIFIED 15a. DECLASSIFICATION/DOWNGRADING SCHEDULE

16. DISTRIBUTION STATEMENT *(of this Report)*

Approved for public release; distribution unlimited.

17. DISTRIBUTION STATEMENT *(of the abstract entered in Block 20, if different from Report)*

18. SUPPLEMENTARY NOTES

Approved for public release; IAW AFR 190-17

Joseph P. Hipps, Major, USAF
Director of Public Relations

19. KEY WORDS *(Continue on reverse side if necessary and identify by block number)*

Imperfections
Rectangular Plates
Collapse

20. ABSTRACT *(Continue on reverse side if necessary and identify by block number)*

An analysis is made of the effect of initial imperfections in geometry on the collapse of simply-supported rectangular plates. A Reissner-type variational principle is employed to evaluate the load versus lateral displacement of elastic, elastic-plastic and orthotropic plates subject to compressive loading along two edges. Imperfection size and shape, plate thickness and aspect ratio, and for orthotropic material, the ply orientation is examined. The results indicate that the load-displacement curve is sensitive to

DD FORM 1 JAN 73 1473 EDITION OF 1 NOV 65 IS OBSOLETE

UNCLASSIFIED

SECURITY CLASSIFICATION OF THIS PAGE *(When Data Entered)*

the initial imperfection, particularly for elastic-plastic materials. The effect of plate size and aspect ratio are similar for all the plates considered with the collapse stresses higher for elastic plates than for elastic-plastic plates. The effect of plasticity becomes insignificant for thin plates when compared with plates with elastic properties. In general, it can be stated that the imperfection function determines the plate's collapse load. For orthotropic plates the effect of ply orientation is significant at aspect ratios less than 1 but relatively insignificant at higher values when comparing the minimum collapse stresses. The difference is dependent upon the magnitude of the ratio of Young's moduli in the major material axes.